THESIS FOR THE DEGREE OF DOCTOR OF PHILOSOPHY

Novel Metal Oxide Bed Materials for Efficient Solid Fuel Gasification and Gas Clean-up in Fluidized Beds

MARTIN KELLER

Department of Chemistry and Chemical Engineering

Division of Environmental Inorganic Chemistry

CHALMERS UNIVERSITY OF TECHNOLOGY

Gothenburg, Sweden 2015

Novel Metal Oxide Bed Materials for Efficient Solid Fuel Gasification and Gas Clean-up in Fluidized Beds

Martin Keller

Gothenburg, Sweden 2015

Department of Chemistry and Chemical Engineering

Division of Environmental Inorganic Chemistry

Chalmers University of Technology

SE-412 96 Gothenburg

Sweden

Telephone + 46 (0)31-772 1000

Cover image:

La, Sr, and Fe-impregnated ZrO_2 bed materials investigated for Chemical Looping Reforming, with increasing Fe content from left to right.

Abstract

In this work the utilization of some novel metal oxide bed materials in dual-fluidized bed gasification systems has been investigated. For this purpose, metal oxide based bed materials can be 1) directly utilized in the dual fluidized bed gasifier (DFB) or in the Chemical Looping Combustion (CLC) process in order to achieve higher gasification rates, or 2) employed in downstream hot gas conditioning processes, e.g. Chemical Looping Reforming (CLR), in order to reform hydrocarbons in the raw gasification gas.

When utilizing such bed materials directly in the primary loop of a DFB gasifier or a CLC fuel reactor, it was shown in this work that the char gasification rate can be increased by different mechanisms. First, the gasification rate can be increased by reducing hydrogen inhibition of the steam gasification reaction. This decrease is caused by the rapid reaction of the metal oxide bed materials with hydrogen produced by the steam gasification. Thus, hydrogen is effectively removed from the vicinity of the gasifying char particle. Second, the gasification rate can be enhanced by the introduction of a potent catalyst for the gasification reaction via the bed material, which is then transferred onto the gasifying char and catalyzes the steam-carbon gasification reaction. This sequence of events has been demonstrated with a Manganese ore that contained Potassium as an effective catalyst for char gasification.

Low-temperature gasification processes such as the DFB process commonly produce a raw gasification gas that is heterogeneous in its composition and that contains, among other contaminants, significant quantities of condensable and non-condensable hydrocarbons. Active metal oxide bed materials can therefore be employed in a hot gas conditioning process such as the CLR process for the purpose of conditioning the raw gasification gas by reforming tars and lighter hydrocarbons. In this work, a large number of transition metal oxides were screened as potential bed materials. Based on the screening results, two promising groups of bed materials for this application were developed. The first group, Cu-impregnated alumina materials, exhibited high degrees of ethylene conversion, but did not reform monoaromatic compounds. The second group, Fe,Sr-doped lanthanum zirconates, achieved high degrees of ethylene and benzene reforming while retaining methane in the gas. The benzene and ethylene conversion could be further improved by co-feeding O_2 with the gasification gas. A benzene conversion of up to 80 % and an ethylene conversion of about 95 % could be achieved at a temperature of 850°C and at a rather high Gas Hourly Space Velocity (GHSV) of 6800 h^{-1}. Considering the expected lower costs and lower toxicity of this material compared to Precious metal- and Nickel-containing catalysts, these metal oxide bed materials are highly promising candidates for application in gasification gas conditioning with the CLR process, in particular when methane is the desired end-product.

Keywords: Gasification, Chemical Looping Combustion, Chemical Looping Reforming, Dual Fluidized Bed, Tar reforming, Hot Gas Clean-up

Acknowledgement

List of publications

This thesis is based on the work presented in the following peer-reviewed papers. They are referred to in the text by Roman numerals and are attached to this thesis.

Paper I

Keller, M.; Leion, H.; Mattisson, T.; Lyngfelt, A., Gasification inhibition in chemical-looping combustion with solid fuels. *Combustion and Flame* **2011,** 158, (3), 393-400.

Paper II

Azimi, G.; Keller, M.; Mehdipoor, A.; Leion, H., Experimental evaluation and modeling of steam gasification and hydrogen inhibition in Chemical-Looping Combustion with solid fuel. *International Journal of Greenhouse Gas Control* **2012,** 11, 1-10.

Paper III

Keller, M.; Leion, H.; Mattisson, T., Mechanisms of Solid Fuel Conversion by Chemical-Looping Combustion (CLC) using Manganese Ore: Catalytic Gasification by Potassium Compounds. *Energy Technology* **2013,** 1, (4), 273-282.

Paper IV

Keller, M.; Leion, H.; Mattisson, T., Thunman, H., Investigation of natural and synthetic bed materials for their utilization in Chemical-Looping Reforming for tar elimination in biomass-derived gasification gas, *Energy & Fuels,* **2014,** 28 (6), pp 3833–3840

Paper V

Keller, M.; Leion, H.; Mattisson, T., Use of $CuO/MgAl_2O_4$ and $La_{0.8}Sr_{0.2}FeO_3/\gamma-Al_2O_3$ in Chemical Looping Reforming System for Tar Removal from Gasification Gas. *accepted for publication in AIChE Journal*

Paper VI

Keller, M.; Fung, J.; Leion, H.; Mattisson, T., Cu-impregnated alumina bed materials for Chemical Looping Reforming of biomass gasification gas. *submitted for publication*

Paper VII

Keller, M.; Leion, H.; Mattisson, T., Chemical Looping Tar Reforming using La/Sr/Fe-containing mixed oxides supported on ZrO_2, *submitted for publication*

Paper VIII

Keller, M.; Leion, H.; Mattisson, T., Chemical Looping Tar reforming with Fe,Sr-doped $La_2Zr_2O_7$ pyrochlore supported on ZrO_2. *submitted for publication*

Contribution report

I. First author, responsible for experimental work, data evaluation and writing.

II. Second author, responsible for part of the experimental work, shared responsibility for data evaluation and writing.

III. First author, responsible for experimental work, data evaluation and writing.

IV. First author, responsible for experimental work, data evaluation and writing.

V. First author, responsible for experimental work, data evaluation and writing.

VI. First author, responsible for part of the experimental work, responsible for data evaluation and writing.

VII. First author, responsible for experimental work, data evaluation and writing.

VIII. First author, responsible for experimental work, data evaluation and writing.

Related peer-reviewed papers not included in this thesis

Arjmand, M.; Keller, M.; Leion, H.; Mattisson, T.; Lyngfelt, A., Oxygen Release and Oxidation Rates of $MgAl_2O_4$-supported CuO Oxygen Carrier for Chemical-Looping Combustion with Oxygen Uncoupling (CLOU), *Energy & Fuels*, **2012**, 26, 6528−6539

Keller, M.; Arjmand, M.; Leion, H.; Mattisson, T., Interaction of Mineral Matter of Coal with Oxygen Carriers in Chemical-Looping Combustion (CLC). *Chemical Engineering Research and Design*, **2014**, 92, 1753–1770

Contents

1. Introduction

The gasification of a variety of solid fuels (biomass, coal, fuels of opportunity like petcoke) presents an interesting and economically viable way of producing either electricity, various chemical intermediates (syngas, synthetic natural gas, methanol, DME, Fischer-Tropsch liquids etc.), heat or a combination of these[1-4]. Gasification of solid carbonaceous fuels can be conducted in a large variety of different gasifiers. As the gasification reactions using steam or CO_2 as gasification agent of solid carbon to produce CO and H_2 are endothermic in nature, heat needs to be supplied to maintain the reactor temperature. This can be achieved either by directly heating the gasifier by supplying oxygen to it and thus utilizing the heat of the exothermic oxidation of carbon, or by heating the gasifier indirectly by providing the heat via a heat transfer medium. The former is commonly referred to as autothermal gasification and the latter as allothermal gasification, and gasification processes can thus be roughly classified according to how the heat is supplied. Many different concepts exist as to how to practically realize autothermal or allothermal gasification[5,6].

Prominent examples of autothermal gasification processes include Moving-Bed processes, Entrained Flow processes and Circulating Fluidized Bed processes[5]. Entrained Flow processes are usually operated at high pressures and high temperatures. The high temperature of gasification enables rapid thermochemical conversion, but, at the same time, limits the maximum achievable chemical energy contained in the resulting syngas, as some of the product gas is inevitably combusted[7]. A further disadvantage of common autothermal gasification processes stems from the necessity of providing oxygen to the gasifier. Oxygen can either be provided pure, which requires a separate Air Separation Unit (ASU), or in the form of air, which leads to a dilution of the product gas with nitrogen and thus a lower heating value of the product gas. When the product gas is combusted to generate electricity the presence of nitrogen can also be cumbersome when the separation of CO_2 from the flue gas is required.

Although allothermal gasification processes are usually designed to operate at rather low temperatures ≤950°C, they do require a heat source of sufficiently high temperature. A process that has been suggested in the 1980s is the utilization of waste heat of hot helium gas from a nuclear High Temperature Reactor (HTR). In this process a heat exchanger is placed within a fluidized bed gasifier, transferring the required heat for gasification[8]. A more recent proposal suggests the utilization of exhaust heat from a Solid Oxide Fuel Cell (SOFC) available at around 900°C, by immersing tubular SOFCs directly in a fluidized bed gasifier[9]. In this concept, termed Super-Integrated Gasification Fuel Cell (S-IGFC), syngas is produced, shifted, cleaned and then utilized in the SOFCs to generate electricity. Another approach is to retrieve some of the char from the gasifier and combust it in a separate reactor

vessel/compartment to generate the heat needed for the gasification. This heat of combustion is then transferred back to the gasifier. As the transfer of this heat from the combustion flue gas to the gasifier directly in a gas/gas heat exchanger within the gasifier would require very large heat exchanger surfaces, alternative concepts for such a heat transfer are required[10]. One strategy is the use of closed tubes called heat pipes, in which a small amount of a liquid is continuously evaporated and condensed, leading to very high heat transfer coefficients and a 10 to 20-fold reduction in required heat transfer area[10]. Another proposed strategy is the use of a solid heat transfer medium. In the Dual Fluidized Bed process (DFB), char is combusted in a fluidized bed and the heat of combustion is transferred onto the bed material (e.g. sand). The hot particles are then circulated to the second fluidized bed, in which their heat is utilized to drive the gasification of the solid fuel[11]. The somewhat colder bed material is then recirculated back to the combustion chamber together with some unconverted char. A variation of this allothermal DFB process is the recently proposed Triple Bed Circulating Fluidized Bed (TB-CFB) process integrated into a so-called Advanced Integrated Gasification Combined Cycle (A-IGCC) plant[12,13]. In such a process, an additional downcomer reactor is envisioned in order to separate the pyrolysis and the gasification[14]. Also, the heat required for gasification is only partly provided by combustion of the char, and is complemented by heat provided by the gas turbine exhaust in order to increase the overall electrical efficiency of the process[13].

Another process which can be considered a variant of the DFB process is the Chemical Looping Combustion (CLC) of solid fuels[15,16]. In this process, the aim is to completely oxidize the fuel in the fuel reactor/gasifier by providing oxygen to the gasifier via the bed material. This can be achieved by choosing appropriate metal oxides as the bed material which are able to take up oxygen during exposure to air, transfer it to the gasifier and utilizing it for the combustion of the fuel. The reduced bed material is then recirculated back to the air reactor where it is reoxidized. Contrary to the DFB process, in CLC it is desired to achieve full conversion of the char in the gasifier and to avoid combustion of the char in the air reactor. The heat needed to drive the gasification reactions is instead obtained from the strongly exothermic oxidation of the bed material in the combustor. The obvious advantage of such a process over other combustion processes is that neither an ASU is required to generate oxygen, nor is the flue gas diluted with N_2. This allows for easier purification of the flue gas to obtain pure CO_2 that can be sequestered or utilized.

In summary, it is observed that the majority of proposed allothermal gasification processes are carried out in fluidized beds and at rather low temperatures $\leq 950°C$ in order to achieve high efficiency and to avoid agglomeration of the bed material. However, the low operating temperature also brings about a number of challenges for the design of the gasification process. Two of the most prominent are 1) to achieve high gasification rates, since at low

temperature, the gasification reaction is kinetically controlled, and 2) to remove or reform hydrocarbons and other contaminants found in the raw product gas.

For both of these challenges, transition metals / metal oxides based bed materials could present a potential remedy. Particular metal / metal oxide pairings or combinations thereof possess catalytic activity or redox properties of interest in the context of addressing these two challenges. These materials can either be employed directly in the gasifier or in a separate reactor system downstream of the gasifier.

In this thesis, such a use of active bed material will be demonstrated by two examples: Challenge 1 is addressed in the context of the DFB and the CLC process, where high char gasification rates at rather low gasification temperatures need to be realized. This can be achieved by the presence of active metal /metal oxide materials in the gasifier, the mechanisms of which will be discussed in Chapter 2 and Papers I-III of this thesis.

Challenge 2 will be addressed in the context of gas cleaning / upgrading of raw gasification gas in a separate downstream unit referred to as Chemical-looping Reforming (CLR). Here, active metal / metal oxides materials are employed in a Dual Fluidized Bed to reform tars and other hydrocarbons, which represent a significant type of contamination of the product gas. This will be discussed in Chapter 3 of this thesis and Papers IV-VIII.

A schematic of the DFB, CLC and CLR processes and their terminology are shown in Figure 1.
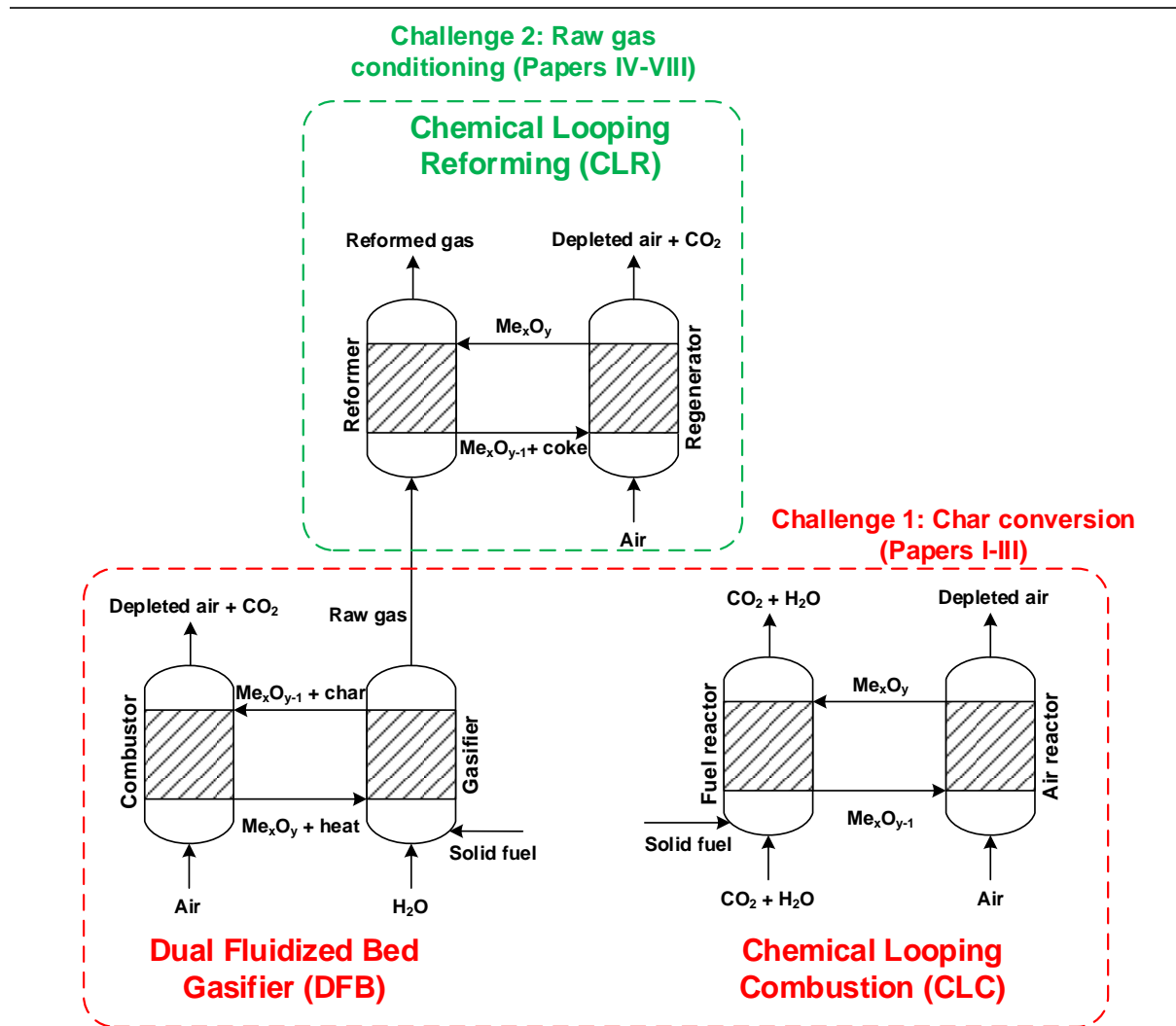
Figure 1: Schematic of the DFB, CLC and CLR processes.

2. Enhancing the char gasification rate in a CLC/DFB gasifier by the use of active metal oxide bed materials

When a wet solid fuel is introduced to a CLC/DFB gasifier, it undergoes three distinct conversion steps. First, it is dried. Upon further heating, it undergoes devolatilization/pyrolysis, in which volatile compounds are released and a solid, carbon-rich residue usually referred to as char is obtained. The fraction of the fuel released as volatiles as well as the nature of the volatile compounds depend on the conditions under which the fuel is devolatilized such as temperature and pressure and the nature of the solid fuel. For coal, the volatile matter content depends on the rank of the coal. Low rank coals such lignite may yield as much as 50 wt-% volatile matter whereas high rank coals such as bituminous coals and anthracites yield significantly lower amounts of volatile matter. The main gaseous products of the devolatilization of coal are C_1 to C_3 hydrocarbons, monoaromatics, light gases such as CO and H_2, and tars[17]. The volatile matter content of biomass may be as high as 80 wt-%[18]. In a third and final step, the char is gasified and the volatile compounds may be further reformed. Either steam or CO_2 can act as gasification agents for the char:

$$C + H_2O \rightarrow CO + H_2 \qquad\qquad (1)$$

$$C + CO_2 \rightarrow 2\,CO \qquad\qquad (2)$$

In comparable reaction conditions (temperature, partial pressure of gasification agent), the steam gasification rate is usually up to one order of magnitude higher than the gasification rate with CO_2 as gasification agent[19]. In this work, the focus will thus be on steam gasification. The rate of char gasification is of great importance in order to achieve a high degree of char conversion at a reasonable residence time of the char in the gasifier. In the CLC process, full conversion of char is desirable. In contrast, in the DFB process, only a certain fraction of the char is to be gasified in order to be able to combust the remaining char for generating the heat necessary for driving the endothermic steam gasification reaction.

In this chapter, the mechanisms of char conversion will be reviewed briefly. Then, measures that have been proposed to increase char conversion in low temperature gasifiers will be discussed, with a focus on the use of active metal oxide bed materials for increasing char conversion. Some experimental results obtained in this context in this work are then briefly summarized.

2.1. Mechanisms of char gasification in a low temperature gasifier

Char gasification with steam as a gasification agent can either proceed non-catalytically or can be catalyzed by a variety of metals. In both cases syngas consisting of CO and H_2 is predominantly formed. Both the catalytic and non-catalytic gasification steps are inhibited by their respective product gases.

2.1.1. Non-catalytic gasification of char

In order to understand the mechanism of non-catalytic char gasification, it is necessary to investigate the steam-carbon reaction more in detail.

The gasification of carbon can be split up in two sequential steps[20]. First, an adsorbed water molecule and a free, active gasification site C_f generate a C(O) surface complex and a hydrogen molecule (oxygen exchange)[20]:

$$C_f + H_2O \xrightarrow{k_1} C(O) + H_2 \tag{3}$$
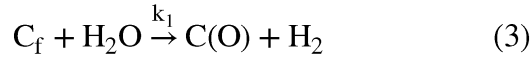
The C(O) surface complex then reacts to gaseous carbon monoxide and a new free, active gasification site (gasification):

$$C(O) \xrightarrow{k_2} CO + C_f \tag{4}$$

According to Hüttinger et al.[21] the hydrogen inhibition of the steam gasification can be described by three different models as elaborated below.

The *oxygen exchange model* is based on the assumption that reaction (3) is reversible:

$$C(O) + H_2 \xrightarrow{k_{-1}} C_f + H_2O \tag{5}$$
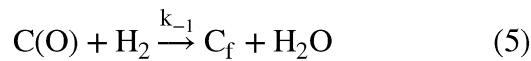
Furthermore, two different models based on hydrogen adsorption have been suggested. The first hydrogen inhibition model assumes *dissociative hydrogen adsorption* on the carbon surface:

$$C_f + \tfrac{1}{2}H_2 \underset{k_{-3}}{\overset{k_3}{\rightleftharpoons}} C(H) \tag{6}$$
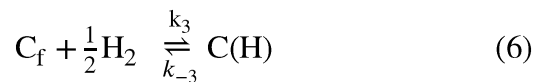
The second hydrogen inhibition model assumes *"associative" hydrogen adsorption*:

$$C_f + H_2 \underset{k_{-4}}{\overset{k_4}{\rightleftharpoons}} C(H)_2 \tag{7}$$
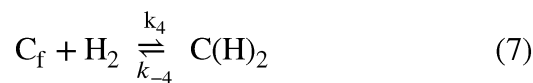
A Langmuir-Hinshelwood type rate expression can be derived for the oxygen exchange model as follows, taking into account eqns. (3) to (5):

$$r_{CO} = k_2 C_{C(O)} \tag{8}$$

$$r_{C(O)} = -k_{-1}C_{C(O)}C_{H_2} - k_2 C_{C(O)} + k_1 C_{C_f}C_{H_2O}(1-\theta) \tag{9}$$

$$\theta = \frac{C_{C(O)}}{C_{C_f}} \tag{10}$$

θ denotes the surface coverage. Assuming steady state

$$\frac{dC_{C(O)}}{dt} = r_{C(O)} = 0 \tag{11}$$

$C_{H_2O} \propto p_{H_2O}$ and $C_{H_2} \propto p_{H_2}$, with c being a lumped constant, yields the expression (12) for the rate of steam-carbon gasification. The rate expressions for the other models can be derived accordingly.

Oxygen exchange model
$$r = \frac{ck_1 p_{H_2O}}{1+\frac{k_1}{k_2}p_{H_2O}+\frac{k_{-1}}{k_2}p_{H_2}} \tag{12}$$

Dissociative hydrogen adsorption
$$r = \frac{ck_1 p_{H_2O}}{1+\frac{k_1}{k_2}p_{H_2O}+\frac{k_3}{k_{-3}}\sqrt{p_{H_2}}} \tag{13}$$

"Associative" hydrogen adsorption
$$r = \frac{ck_1 p_{H_2O}}{1+\frac{k_1}{k_2}p_{H_2O}+\frac{k_4}{k_{-4}}p_{H_2}} \tag{14}$$

As equations (12) and (14) are formally identical, it is more complicated to distinguish between these two inhibiting effects.

It is believed that the inhibition due to the oxygen exchange model, equation (5), and the inhibition due to the formation of $C(H_2)$ complexes, equation (7), are reversible[20,21]. A permanent reduction of the number of free, active gasification sites by these inhibition mechanisms is therefore omitted and the rate of gasification of carbon depends solely on the current hydrogen partial pressure in the reactor[21].

In the past, a number of researchers have observed hydrogen inhibition of the steam gasification reaction that follows an LHHW rate expression with a square root dependency on

the hydrogen partial pressure and therefore inhibition due to the formation of C(H) complexes[21-24]. The C(H) surface complexes were found to be stable and therefore the hydrogen inhibition was assumed to be irreversible[21].

The reversible or irreversible nature of the H_2 inhibition was, however, explicitly investigated by only few authors[20,21]. Hüttinger et al.[21] conducted gas exchange experiments and gasification experiments with H_2-pretreated carbon and observed a large irreversible H_2 inhibition. Lussier et al.[20] observed an irreversible H_2 inhibition only at the very beginning of the gasification process and could not observe irreversible inhibition in gas exchange experiments.
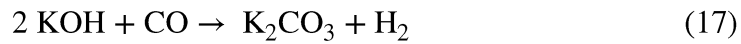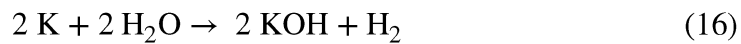
Since the rate equations for the oxygen exchange model and the associative hydrogen adsorption model have the same mathematical structure, distinguishing between these two models is somewhat complicated. Lussier et al.[20] have investigated the hydrogen inhibition for steam/hydrogen gasification using temperature programmed desorption (TPD) for annealed Saran char. The authors showed that associatively adsorbed hydrogen is completely desorbed at temperatures above 727°C during TPD. Consequently, associative hydrogen adsorption should not be present at temperatures higher than 727°C and therefore should not inhibit the reaction. Thus, it can be concluded that at higher temperatures the oxygen exchange mechanism is likely to inhibit the gasification reaction[20].

2.1.2. Catalytic gasification of char

The gasification of carbon can be catalyzed by a broad range of inorganic constituents, the most active being transition metals, alkali metals and alkaline earth metals[25]. Their activity depends on the gasifying conditions, the gasifying agent (in this case steam) and the dispersion of the catalyst. Nishiyama suggested the classification of catalysts for the carbon gasification reactions into three distinct groups based on their observable influence on the resulting catalytic gasification behaviour. He classified the catalysts into the alkali metal group, the alkaline earth metal group and the iron group, containing Ni and Fe[26]. Mims suggested a classification based on catalyst morphology and thus its mode of attack on the carbon surface. That is, the strength of the interfacial attraction of the catalyst and the carbon surface determines the wetting tendency. Thus, catalysts with weak interfacial attraction tend to form discrete particles resulting in a channelling mode of catalytic attack. On the other hand, catalysts with strong interfacial attractions tend to form thin films resulting in edge recession as the dominant mode[25]. A channelling mode of attack has been observed for transition metals such as Ni, Fe and V whereas an edge recession mode has been observed for alkali and alkaline earth metals such as K and Ca[25]. As the initial dispersion of the catalyst is crucial for the effective catalysis, the method by which the catalyst is introduced into the fuel is of relevance. Often times the catalyst is introduced to the solid fuel by wet impregnation[27].

Out of the potential catalysts, the alkali metal group, in particular potassium, has been researched most extensively. This is due to the abundance of potassium in the earth's crust and thus its low price and the high activity it exhibits towards the gasification of coal[25–28]. The mechanisms and kinetics of alkali metal catalyzed gasification have therefore been investigated thoroughly by a number of researchers. It was found that the main mechanism of catalysis involves the supply of oxygen from the catalyst to the carbon. McKee et al. proposed a catalytic cycle initiated by the carbothermic reduction of the alkali carbonate[29]. For the K-catalyzed steam-carbon reaction the suggested catalytic cycle can be written as follows:

$$K_2CO_3 + 2\,C \rightarrow 2\,K + 3\,CO \qquad (15)$$

$$2\,K + 2\,H_2O \rightarrow 2\,KOH + H_2 \qquad (16)$$

$$2\,KOH + CO \rightarrow K_2CO_3 + H_2 \qquad (17)$$

Mims and Pabst[30] proposed a rate equation for the catalyzed steam gasification analogously to the rate equation for the uncatalyzed steam gasification reaction, which also includes a hydrogen inhibition term.

$$r_{C+H_2O,\,\text{catalyzed}} = k_3\,\frac{p_{H_2O}}{p_{H_2O} + k_4 p_{H_2}} \qquad (18)$$

Meijer et al. derived more complex kinetics for the alkali catalyzed steam gasification and observed, additionally to H_2 inhibition, severe gasification inhibition by CO[31].

Many solid fuels that can be utilized in low temperature gasification processes such as coal, in particular lignite, and biomass can already contain rather large quantities of alkali metals such as Na and K, either bound in mineral matter or bound to the organic structure of the fuel. These can exhibit catalytic activity towards the steam-carbon gasification reaction and thus lead to an inherently increased char gasification rate[32].

2.2. Measures to increase char conversion in a low temperature gasifier

In the low temperature steam gasification of solid fuels in fluidized beds, the operating temperature is constrained either by a desire to maintain a high cold gas efficiency of the gasification process or by fuel-related ash softening or agglomeration issues. For a given fuel at a given temperature and pressure, an increase in char conversion in the gasifier can then be achieved either by increasing the rate of char gasification or by increasing the residence time of the char in the gasifier. This can be practically realized by either changing the physical layout of the gasifier, by altering the fuel prior to its introduction into the gasifier or by using an active bed material. An attempt at categorizing proposed measures to increase char conversion according to these classifications is shown in Table 1.

Table 1: Overview and categorization of some proposed measures to increase char conversion

	Increasing avg. char residence time	Increasing gasification rate

Design optimization	• Change of solid fuel flow pattern in gasifier by
	  o insertion of internals (tubes, baffles)[33]
	  o installing Carbon stripper[34,35]
		• Separating gasification and pyrolysis
		  o Triple-Bed CFB with downcomer[14]
		  o Dong et al. concept[36]
		  o VIKING gasifier[37]

Alteration of fuel		• Impregnation of catalyst on
		  o raw fuel[27]
		  o demineralized fuel (e.g. HyperCoal process)[38]

Use of active bed material		• Decreasing H_2 inhibition (Paper I+II) • Catalyzing gasification by in-situ transfer of catalyst from bed material to char (Paper III)

Average char residence time can be potentially improved by design measures that alter the flow of the solid fuel through the gasifier. For the DFB process, the insertion of internals such as tubes and baffles has been suggested and investigated[33]. For the CLC process the residence time of the fuel in the gasifier / fuel reactor has been shown to be significantly increased by the installation of a Carbon stripper[34,35]. In such a Carbon stripper, the unconverted char is separated from the bulk bed material particles by exploiting the difference in terminal velocity of the char and the bulk bed material as a consequence of a difference in density and/or particle size[34,35]. The unconverted char is then reintroduced to the gasifier / fuel reactor, whereas the bulk bed material is circulated back to the combustor (see Figure 1).

An increase in gasification rate can be achieved by constructive measures that separate the char gasification and the pyrolysis physically in order to avoid exposure of the char to volatiles generated during the pyrolysis. It has been demonstrated that such an exposure leads to a decrease in char reactivity[39]. The reason for this decrease is believed to be that the steam reforming of volatiles generates hydrogen radicals which then induce a condensation of aromatic ring systems in the char, leading to its graphitization[40]. Many different reactor designs have been proposed to avoid such volatile-char interactions. Matsuoka et al. proposed a Triple Bed Circulating Fluidized Bed (TB-CFB), in which an additional downcomer reactor is installed in which the fuel is pyrolyzed and then the char is introduced to the gasifier[14,41,42]. In the VIKING gasifier, the fresh fuel is first pyrolyzed and the volatiles are then partially oxidized at high temperature, and that gas is then used to gasify the remaining char[37]. Dong et al. proposed a reactor concept with a counter-current flow of solid fuel and gas in which the fuel is thought to be devolatilized before it reaches the char bed[36].

As described in section 2.1, the char gasification rate can also be increased by impregnating the fuel with an effective catalyst prior to its introduction into the gasifier. Either the raw fuel can be impregnated directly, or the fuel can be pre-treated by acid-leaching of ash forming minerals[43]. Ash-free coal termed "HyperCoal" impregnated with K_2CO_3 has been shown to achieve even higher rates of gasification than raw coal impregnated with K_2CO_3 due to the avoidance of deactivation of the catalyst by the interaction with mineral matter contained in the raw coal[38]. However, both of these options require the treatment of all of the fuel that is to be gasified, which may result in high costs due to the large mass flow of fuel.

Finally, the gasification rate of the char may also be increased by using a fluidized bed constituted of active bed material in the gasifier. In the work presented in this thesis, this approach of increasing char conversion was pursued. Two different ways in which an active bed material can increase the gasification rate were investigated. First, an oxidized metal oxide bed material could provide lattice oxygen to convert some or all of the product gases of the steam-carbon reaction, which would result in a decrease of the H_2 concentration in the environment in which the char is gasified. As discussed in section 2.1, H_2 is a potent inhibitor of the char gasification reaction. In Papers I and II of this thesis the effect of H_2 removal on the inhibition of the char gasification is discussed and experimentally quantified. In these papers, this effect is studied at rather low hydrogen pressures that are to be expected in the vicinity of active metal oxide bed materials. A second way of increasing char gasification rate considerably by using active bed materials is the introduction of a catalyst via the bed material to the gasifier. This is discussed and demonstrated for a Manganese ore in Paper III.

2.2.1. Decreasing H₂ inhibition by use of active bed material

The decrease of H_2 inhibition due to the removal of H_2 by reaction with an oxidized active metal oxide bed material is of interest and has been investigated both in the context of CLC and in the context of DFB gasification. As solid-solid reactions between the char and such an active metal oxide bed material do not occur at an appreciable rate, the char is first gasified by steam according to equation (1). Subsequently, the resulting syngas is further oxidized by reacting with the active metal oxide bed material:

$$CO + Me_xO_y \rightarrow CO_2 + Me_xO_{y-1} \qquad (19)$$

$$H_2 + Me_xO_y \rightarrow H_2O + Me_xO_{y-1} \qquad (20)$$

Analogously, volatiles evolved during devolatilization of the fuel may be oxidized by the bed material. For CLC, the decrease of H_2 inhibition is an inherent feature of the process. H_2 evolving from the fuel devolatilization and char gasification will be oxidized by the metal oxide bed material according to equation (20), thus decreasing the partial pressure of H_2 in the reactor. For DFB gasification, only partial oxidation of the syngas is desired at most, and, while a partial oxidation of H_2 by the bed material may yield higher char conversion, it simultaneously reduces the cold gas efficiency of the gasification process. This interplay has been investigated in greater detail by Larsson et al[44].

Experiments were carried out in this work to demonstrate the applicability of the hydrogen inhibition concept to char gasification in the vicinity of an oxidized active metal oxide bed material. Further experiments were conducted to determine the predominant hydrogen inhibition mechanism, to determine its reversibility or irreversibility and to quantify this effect.

Details of the design of the experiments and the experimental setup are described in Paper I and Paper II of this work. In these experiments small batches of different solid fuels were converted with steam in small fluidized bed reactors in the presence of diverse metal oxide bed materials. The applicability of the hydrogen inhibition concept was shown by connecting the observed gasification rate to the hydrogen partial pressure in the reactor. In this way the reaction kinetic rates have also been quantified as a function of the hydrogen and the steam partial pressure. It was found that the hydrogen inhibition of the steam-carbon reaction could best be described by a linear dependence of the inhibition term on the hydrogen partial pressure corresponding to either the oxygen exchange model, equation (12), or the associative hydrogen adsorption model, equation (14).

To determine the irreversibility of the hydrogen inhibition, experiments have been carried out in which wood char particles were pretreated at 970°C with either 30 mol-% H_2 in N_2 or pure

nitrogen before their gasification. The results of these experiments are shown in Figure 2. These results did not indicate a significant change in gasification rate when the char particles are pretreated with hydrogen, even after a long pretreatment time of 60 minutes. The small changes in gasification rate that could be observed can be attributed to experimental variations. Thus, under the given experimental conditions, an irreversible hydrogen inhibition could not be observed even after a rather long exposure of the char particles to H_2. Since the formation of C(H) complexes was found to be irreversible by other researchers, hydrogen inhibition due to the formation of such complexes appears unlikely as the predominant mechanism of hydrogen inhibition.
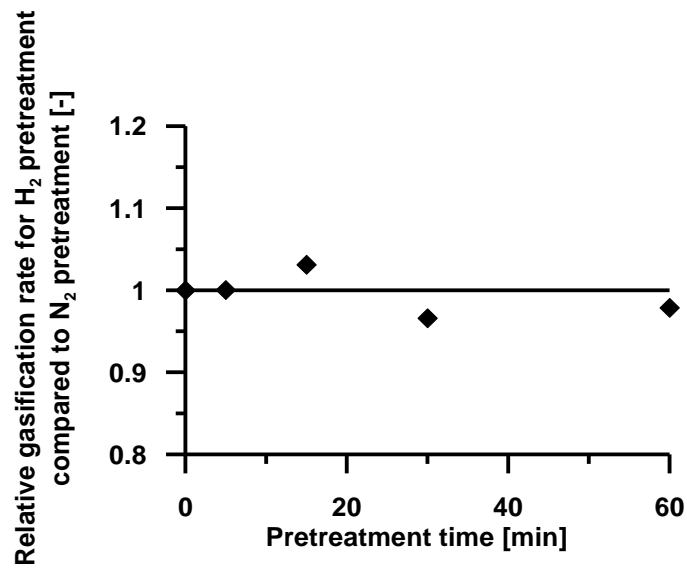
Figure 2: The relative change of gasification rate for H_2 pretreatment compared to N_2 pretreatment for different pretreatment times. (♦): experimental values.

As discussed in section 2.1, a distinction between the oxygen exchange model and the associative hydrogen adsorption model is complicated due to the identical structure of the rate equations. However, based on the analysis by Lussier discussed in section 2.1, it can be concluded that for temperatures relevant for low-temperature gasification processes above 727°C, the oxygen exchange mechanism is likely the dominant mechanism of inhibition of the char gasification reaction.

The obtained reaction kinetics can be utilized to plot the expected gasification rate as a function of hydrogen and steam partial pressure. This is shown in Figure 3 and Figure 4 for two different fuels, a Swedish wood char and a Colombian bituminous coal at 970°C.
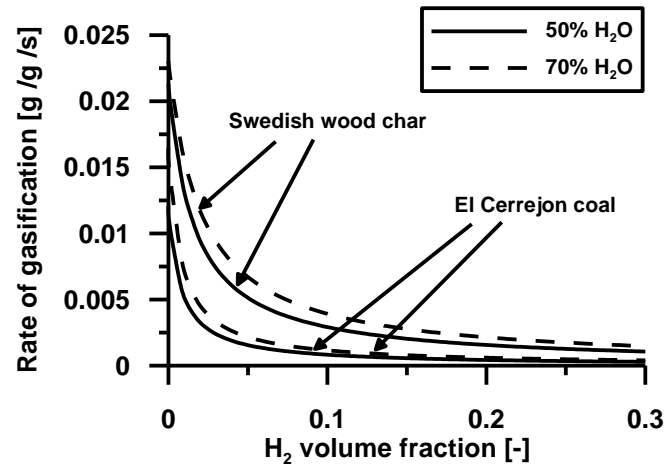
Figure 3: Prediction of the rate of conversion as a function of hydrogen volume fraction for steam gasification of Swedish wood char and El Cerrejon coal in 50% and 70% steam.
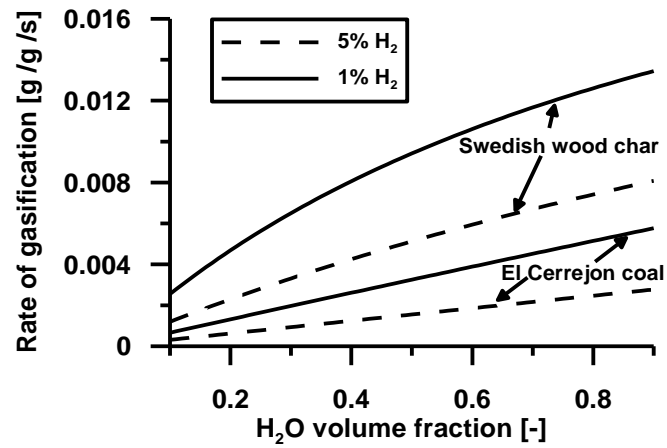

Figure 4 Prediction for the rate of conversion of Swedish wood char and El Cerrejon coal as a function of steam volume fraction for 5 % and 1% hydrogen volume fraction.

2.2.2. Catalyzing gasification by in-situ transfer of catalyst from bed material to char

Apart from increasing the gasification rate by decreasing the H_2 concentration in the vicinity of the char, an increase in gasification rate can be also achieved by catalyzing the steam gasification of char. This can be achieved by using a bed material which is able to release catalytically active elements in the gasifier that can be adsorbed by the char and then catalyze its gasification.

In previous research it has been observed that for several solid fuels very high char gasification rates can be achieved when the char is gasified in a bed of Brazilian Manganese ore. The observed apparent gasification rates for a petroleum coke were as much as five times higher than rates observed in an ilmenite bed and almost ten times higher than rates observed in a sand bed[45,46]. Furthermore, it was observed that the rate of char gasification in a bed of Brazilian manganese ore greatly exceeded those seen in a bed of synthetic manganese oxide particles[47]. This indicated that a decrease in H_2 inhibition due to high reactivity of Manganese towards syngas cannot be responsible for the drastic increase in gasification rate. Thus, in Paper III of this thesis, the mechanisms of char conversion in the presence of this bed material were investigated in more detail. In order to omit any influence of the conversion of volatiles on the char conversion and to make catalyst transfer from the bed material observable, petroleum coke was chosen as a model fuel because it has a very low volatile matter content and it contains no catalytically active alkali metals. With this fuel, partial gasification experiments were conducted. In these partial gasification experiments batches of petroleum coke particles were inserted into a fluidized bed consisting of quartz sand (for reference) and into a fluidized bed consisting of Brazilian Manganese ore. The particles were then partially gasified in 50 % H_2O in N_2, and the gasification reaction was then interrupted by cooling down the reactor rapidly in a flow of pure N_2. Both batches of partially gasified petroleum coke particles as well as a batch of fresh petroleum coke particles were then analyzed with a Scanning Electron Microscope (SEM) and by Energy-dispersive X-ray spectroscopy (EDX). EDX mapping revealed that the particles gasified in the manganese ore fluidized bed contained significant quantities of potassium (about 0.3 wt-%), whereas potassium could not be detected in either the fresh petroleum coke or the petroleum coke gasified in a sand bed. This proved the occurrence of a transfer of potassium from the manganese ore bed material to the petroleum coke particles during the fuel conversion process. EDX mapping of the cross-sections of fuel particles gasified in the manganese ore also demonstrated that the potassium was well and almost uniformly distributed throughout the particle. This shows a high mobility of the potassium from the manganese ore to the fuel and may thus indicate a potassium transport via the gas phase.

Although the observed quantity of K of about 0.3 wt-% seems small, effective catalytic gasification by potassium has been observed previously at low potassium concentrations of 1 wt-% by other authors[48]. When employing a wet impregnation method the formation of alkali metal carbonate crystals is likely to occur, which hinders the dispersion of the alkali metal[27]. In the experiments discussed in this work, the transfer of K to the particle occurs at high temperatures and likely via a gas-phase compound. As a consequence, the dispersion of K throughout the particle can be expected to be significantly improved in comparison to wet impregnation methods. Thus, the relatively small absolute quantities of K detected may be sufficient for effective gasification catalysis.

SEM/EDX analyses of particle cross-sections of both fresh manganese ore and used manganese ore revealed that the ore contains K-Al-Si-rich inclusions that have a composition which corresponds approximately to a Kalsilite-like structure ($KAlSiO_4$). The Potassium transferred onto the fuel is thus likely to originate from these Kalsilite-like inclusions in the ore.

3. Chemical Looping Reforming (CLR) with active metal oxide bed materials

In contrast to high-temperature gasification processes, low-temperature gasification processes such as the DFB process produce a raw gas which is highly heterogeneous in its composition[49–51]. In Table 2 the gas compositions of several DFB gasifiers with biomass as fuel are shown.

Table 2: Gas composition and approximate energy content of raw gasification gas from three different DFB gasifiers

	Chalmers gasifier[49]		FICFB gasifier[51]		MILENA gasifier[50]	
Fuel used	Wood pellets		Softwood pellets		Beech wood chips	
Bed material	Sand		Olivine		Sand	
$T_{gasifier}$ [°C]	830		803		851	
H_2O [mol-%]	50.71		47.5		39	
	mol% db	% energy*	mol% db	% energy*	mol% db	% energy*
H_2	21.02	16	35.3	29	24.9	18
CO	35.35	26	29.1	24	28.8	21
CO_2	14.47		17.3		20.4	
CH_4	12.85	30	11.1	28	11.7	27
C_2H_x	5.26	20	3.5	14	4.9	18
BTX	n.d.	n.d.	n.d.	n.d.	1.2	10
N_2	11.06		1.2		6.2	
	g/m^3_N db					
Tars	32.89	8	17.7	5	27.8	6

*Assumptions for calculating energy content: C_2H_x as ethylene, BTX as benzene, tars as naphthalene.

Apart from the main syngas components CO and H_2, the raw product gases contain substantial amounts of hydrocarbons. The CH_4 content is around 11-13 mol-%(db), the C_2H_x content around 3-5 mol-%(db), the monoaromatics (benzene, toluene, xylene) content up to 1.2 mol %(db) and the content of heavier, condensable hydrocarbons commonly referred to as "tars" is about 10-30 g/m^3_N (db). The already high CH_4 content of the raw gas of these DFB

processes makes it especially attractive for the production of Substitute Natural Gas (SNG) in a downstream methanation process. It should be noted that the high content of hydrocarbons in the gas originates mainly from the high volatile matter content of biomass, and when using lignite as a fuel in a DFB process, a considerably lower fraction of hydrocarbons is to be expected[52,53]. When the composition of the raw gas with woody biomass as a fuel is expressed as energy content of the combustible components, it can be observed that only about 40-55 % of the energy is contained in the main syngas compounds, about 30 % in the form of CH_4, about 15-20 % in the form of C_2 hydrocarbons, up to 10% in the form of benzene, toluene and xylene (BTX) and about 5-8 % in the form of tars. The high energy content of these hydrocarbons incentivizes the application of gas conditioning strategies that do not simply remove them from the gas stream, but instead recover them as useful byproducts or reform them to compounds whose chemical energy can be utilized in downstream synthesis steps. Thus, these hydrocarbons, together with other impurities such as sulphur compounds and ammonia, require a considerable gas cleaning and conditioning effort downstream of the gasifier when this gas is to be utilized for combustion or in the synthesis of fuels such as SNG in an efficient fashion. Especially cumbersome are tars as they start condensing already at rather high temperatures which may cause operational problems such as fouling and blocking of downstream equipment[54]. Apart from tars and hydrocarbons, sulfur species are also cumbersome when a fuel synthesis is to be conducted, as sulfur is a potent poison for Nickel-based methanation catalysts already at very low concentrations[55]. Raw biomass gasification gas usually contains sulfur in the form of H_2S, COS and organic sulfur compounds such as thiophene (C_4H_4S)[56,57].

When the objective is to produce SNG, a gas conditioning system should thus ideally be able to fulfill the following targets with as few unit operations as possible:

- Retain CH_4 in the gas as it is the desired product.
- Completely convert/remove tars and all other hydrocarbons except CH_4. Ideally, the chemical energy of the hydrocarbons would at least partially be retained by reforming hydrocarbons to either syngas or directly to CH_4.
- Remove all sulfur species from the gas, including H_2S, COS and organic sulfur.
- Remove NH_3 and HCl from the gas.
- Adjust the concentrations of H_2, CO and CO_2 so that the feed gas module $M = \frac{x_{H_2} - x_{CO_2}}{x_{CO} + x_{CO_2}}$ is equal to 3. This can be achieved via the water gas shift reaction and/or the separation of CO_2.

Generally, it is more desirable to conduct gas cleaning and conditioning at temperatures between the gasifier outlet temperature and the inlet temperature of the catalytic synthesis process (around 300°C for the methanation process). When low temperature gas conditioning

steps are conducted, the gas needs to be reheated again to the temperature required in subsequent synthesis steps, such as the methanation. When all the gas conditioning steps are conducted at temperatures higher than or equal to the inlet temperature of the synthesis process, such a reheating can be avoided.

For the removal of sulfur compounds from the gasification gas, different strategies need to be pursued when hot gas cleaning is desired as compared to cold gas cleaning. When biomass is used as fuel, the gasification usually contains sulfur predominantly in the form of H_2S (50-200 ppm), with smaller quantities of COS and organic sulfur also present[58]. In a typical low-temperature gas conditioning configuration, organic sulfur and COS are first hydrogenated to H_2S in a catalytic hydrodesulfurization reactor (HDS), the H_2S is then removed in a scrubber and residual sulfur species are finally captured in a guard bed. When the sulfur removal is to be conducted at higher temperatures $\geq 300°C$, solid sorbents that are able to bind sulfur need to be utilized[59,60]. ZnO-based sorbents exhibit favorable properties for sulfur removal from gasification gas, and are currently evaluated for sulfur removal from a coal gasification gas at an IGCC power plant at a 50 MW_e scale[61]. However, while ZnO-based sorbents are able to reduce H_2S and COS concentrations to sub-ppm levels, they are not able to adsorb organic sulfur compounds such as thiophene[56]. As a consequence, an HDS unit would still be required upstream of a ZnO sorbent bed when very low sulfur levels need to be realized. Mn-based sorbents have also been evaluated for hot gas desulfurization of gasification gas, however only with H_2S as sulfur compound[62-64]. Recent experimental results obtained at Chalmers University of Technology indicated that these materials are not able to remove organic sulfur compounds from the gas.

For the removal or reforming of tars and hydrocarbons from the gasification gas, numerous approaches have been suggested. They can be categorized as primary measures conducted directly inside the gasifier or secondary measures conducted downstream of the gasifier in separate unit operations[58,65]. One suggested primary measure is the use of active bed materials in the DFB gasifier. As seen in Table 2, the use of olivine as a bed material in the FICFB gasifier reduces the amount of tars and C_2 hydrocarbons significantly[66]. However, primary measures are limited in their efficiency, mainly due to the limited contact time between the bed material and gases evolving from the fuel. Secondary measures allow for greater flexibility in process parameters such as operating temperature and additional steam injection, and a well-defined residence time of the gas offers the potential of achieving a higher degrees of gas conversion[58,65].

Secondary measures can either be conducted at low temperatures (e.g. scrubbing with water, oil or other solvents, active carbon filters) or at medium to high temperatures. As already mentioned, hot gasification gas conditioning is desirable when the gas is used in high-temperature synthesis processes downstream of the gas cleaning. However, many catalytically

active materials investigated for hot gasification gas conditioning suffer from deactivation due to the formation of coke and the adsorption of sulfur on the catalytically active surface. This is particularly problematic when they are used in reactor configurations in which they are continuously exposed to the raw gasification gas[67,68]. As a potential remedy for such deactivation, reactor configurations have been recently proposed that circumvent this problem by continuously regenerating the catalyst in a similar way as it is conducted in a Fluid Catalytic Cracking (FCC) unit[69,70]. In such a process, the gas conditioning is envisaged to be realized in a dual-fluidized bed reactor system. The bed material is circulated between a reformer, in which the bed material is contacted with the raw gasification gas, and a regenerator, in which the bed material is regenerated by oxidizing coke deposits and sulfides with air. Throughout this thesis this process is referred to as Chemical Looping Reforming (in short CLR)[69]. This proposed process and its terminology are illustrated in Figure 1 in section 1. An overview of plausible hydrocarbon reaction pathways in the CLR process can be found in Paper IV appended to this thesis. In the CLR process the degree of oxidation of the raw gas is determined by the amount of oxygen transported by the bed material from the regenerator to the reformer. The degree of oxidation may thus be controlled by the oxygen carrying capacity of the bed material, the recirculation rate of the bed material or by providing an understoichiometric amount of oxygen to the regenerator.

For the CLR process, the selection of an appropriate bed material is essential. The aim of the work conducted for this thesis was thus to identify, test and improve suitable bed materials that perform well with respect to the conversion of tars and other hydrocarbons.

The vast body of literature on tar removal or reforming from raw gasification gas in fixed bed reactor configurations shall serve as a starting point for the identification of promising bed materials for CLR. An overview and categorization of these materials has been presented by El-Rub et al.[71].

Calcined rocks containing alkaline earth metal oxides such as CaO and MgO have received much attention because they exhibit high degrees of tars conversion[72–79]. They can be produced by calcining carbonate rocks such as limestone, calcite or dolomite. They were found to be capable of steam reforming C_2 to C_4 hydrocarbons and even monoaromatics such as benzene[74,80], compounds which are notoriously difficult to convert. At the same time, calcined rocks retain CH_4 in the syngas, which would be advantageous if CH_4 is the desired product[75]. It was observed that coke formation leads to deactivation of the calcined rocks by covering their active sites and blocking pores[67,75]. Due to their high activity for tar reforming, their inexpensiveness and their abundance, these materials appear attractive for use in CLR as the deactivation by coke formation could potentially be overcome by continuous regeneration. However, the softness and brittleness of these materials results in high attrition rates when used in fluidized beds[75]. Calcined rocks were thus not further considered for use in CLR.

Char produced by the pyrolysis of coal or biomass has also attracted considerable attention for its tar removal capabilities recently[81,82]. It has been observed that char exhibits high activity towards the conversion of tar compounds in gasification gas[81]. Generally, the conversion of aromatics over char increases with the number of aromatic rings per molecule, and the conversion of benzene is thus most difficult to achieve[83]. Nevertheless, in the presence of steam and H_2 high degrees of benzene conversion >60% were observed at T=850°C[83]. Aromatics were mainly decomposed to coke, and the gasification rate of coke needs to be high enough to maintain catalytic activity[81,83]. Chars or char as support for metal impregnated catalysts are, however, unsuitable as bed materials in CLR since they would easily be combusted when exposed to oxygen-rich gas in the regenerator.

Solid acid catalysts, and in particular zeolites, have also been investigated for tar removal from gasification gas[84]. A naphthalene conversion of up to 55% was observed at T=750°C over ultra-stable Y zeolites (USY)[84]. Since rare-earth exchanged USY zeolite constitute the catalytically active part of FCC catalyst formulations, the use of commercially available FCC catalysts for tar removal appears plausible[85]. In the "Therminator" process, whose layout is similar to the CLR process, a mixture of $ZnTiO_3$ sulfur sorbent and commercial FCC catalyst was used as the bed material at a temperature of 600°C. The acidity of the FCC catalyst causes fairly high degrees of tar cracking to form coke, which is then combusted in the regenerator. H_2S is chemisorbed to form ZnS, which is then oxidized in the regenerator to form SO_2. CH_4 and C_2 hydrocarbons are neither converted nor removed in this process[70]. Because of the inability to convert lighter hydrocarbons and the limited operating temperature as a result of hydrothermal instability of USY zeolite, FCC catalysts were not investigated as bed materials in CLR.

Platinum group metals such as rhodium, ruthenium and iridium were found to be particularly active for CH_4 steam reforming[86]. As a consequence, they attracted some interest for their use in gasification gas conditioning as well. Similar trends were observed in biomass gasification gas cleaning, with rhodium and iridium generally being the most active in the steam reforming of aromatic compounds such as benzene[87–91]. Due to their very high activity for hydrocarbon reforming, rhodium and iridium containing catalyst convert not only tars and BTX, but also lighter hydrocarbons such as ethylene[87]. From the viewpoint of catalytic activity, these catalysts appear thus highly attractive for utilization in gasification gas conditioning. However, the high price of platinum group metals is an issue, especially when the catalyst is to be used in a fluidized bed in the CLR process, where loss of catalyst due to attrition and intermixing with dust from the gasifier can be expected. Therefore, platinum group metals containing catalysts were not investigated as bed materials in CLR either.

Instead, the focus has been put on first-row transition metal containing bed materials. Naturally occurring ores, waste materials and synthetic catalyst were considered. At Chalmers

University of Technology the CLR process has been tested for gasification gas conditioning in a continuous unit. Ilmenite natural ore [69,92], a Manganese natural ore[93], Mn_3O_4 supported on ZrO_2[49] and NiO supported on α-Al_2O_3[92,94] have been investigated as bed materials. With ilmenite and the Mn-containing materials, a decrease of the total mass of tars was observed, but CH_4, aromatic compounds and C_2 hydrocarbons were not converted efficiently. The Ni catalyst was able to convert tars, C_2 hydrocarbons, aromatic compounds and some CH_4. However, the utilization of Ni- or Co-containing catalysts is problematic as they pose a health risk when used in a fluidized bed due to the formation of breathable dust because of particle attrition.

The aim of the work was thus to identify, synthesize and investigate bed materials containing first-row transition metal / metal oxides other than Ni or Co for their use in gas conditioning of raw gasification gas in the CLR process. To this end, an experimental setup was constructed in which bed materials can be investigated; in particular their transient behavior when being exposed to reducing and oxidizing conditions as they would be exposed to in a CLR unit. Flue gas compositions were analyzed by FT-IR with a high time resolution. Ethylene, toluene and benzene were used as tar surrogates in a synthetic gasification gas matrix. Not only are they interesting as tar surrogates, but the fate of ethylene and monoaromatics is also of great relevance due to their high concentrations and energy content in the raw gas as shown in Table 2. In all CLR experiments conducted in this work, the tested bed material was alternatingly exposed to reducing and oxidizing conditions in order to emulate the circulation of the bed material between the regenerator and the reformer of a continuous CLR unit. The bed material was exposed to gasification gas for 1000 seconds and to air for 360 seconds to allow for full reoxidation of the bed material. In between these exposures, the reactor was flushed with N_2. The system was operated at atmospheric pressure and the temperature was varied between 600°C and 850°C. The composition of the synthetic gasification gas used in the different experiments are shown in Table 3. Further details regarding the experimental setup and procedure are described in Paper IV.

Table 3: Synthetic gasification gas compositions used throughout the CLR experiments described in this thesis

Conc. in mol-%	Screening with C_2H_4 (Paper IV)	Ethylene, toluene and benzene reforming experiments (Paper V)	Ethylene and benzene reforming experiments (Papers VI, VII, VIII)	Selective Catalytic Oxidation experiments (Papers VII, VIII)
H_2O	40	25	25	25
CO	17.2	10.75	10.75	10.75
CO_2	5.96	3.73	3.73	3.73
H_2	9.25	5.78	5.78	5.78
CH_4	5.6	3.5	3.5	3.5
C_2H_4	1.99	1.25	1.25	1.25
C_6H_6	-	$0 - 1.4\,\%$	$0 - 1.4\,\%$	$0 - 1.8\,\%$
C_7H_8	-	$0 - 1.4\,\%$	-	-
O_2	-	-	-	$0 - 2.5\,\%$
N_2	balance	balance	balance	balance

In Paper IV of this thesis the results of a screening study conducted with ethylene are presented. Here, a large number of materials were tested, both natural and synthetic oxides. In Paper V further results with toluene and benzene for two bed materials that were identified as very promising for their application in CLR are reported on. The focus of Paper VI is on the conversion and properties of Cu-containing bed materials and the influence of choice of support. Finally Papers VII and VIII report promising results obtained with La/Fe/Sr-impregnated ZrO_2 support materials.

Raw gas concentration profiles of experiments conducted are not shown in this thesis, but can be found in Papers IV, V, VI and VII.

3.1. Screening of first-row transition metal / metal oxides containing bed materials for use in CLR

A screening study was conducted in order to determine the suitability of different first-row transition metal oxides containing bed materials for CLR. C_2H_4 was used as a tar surrogate in a synthetic gasification gas resembling raw gas from a DFB process (see Table 3). In Table 4 the composition and production parameters of the synthetic particles are summarized.

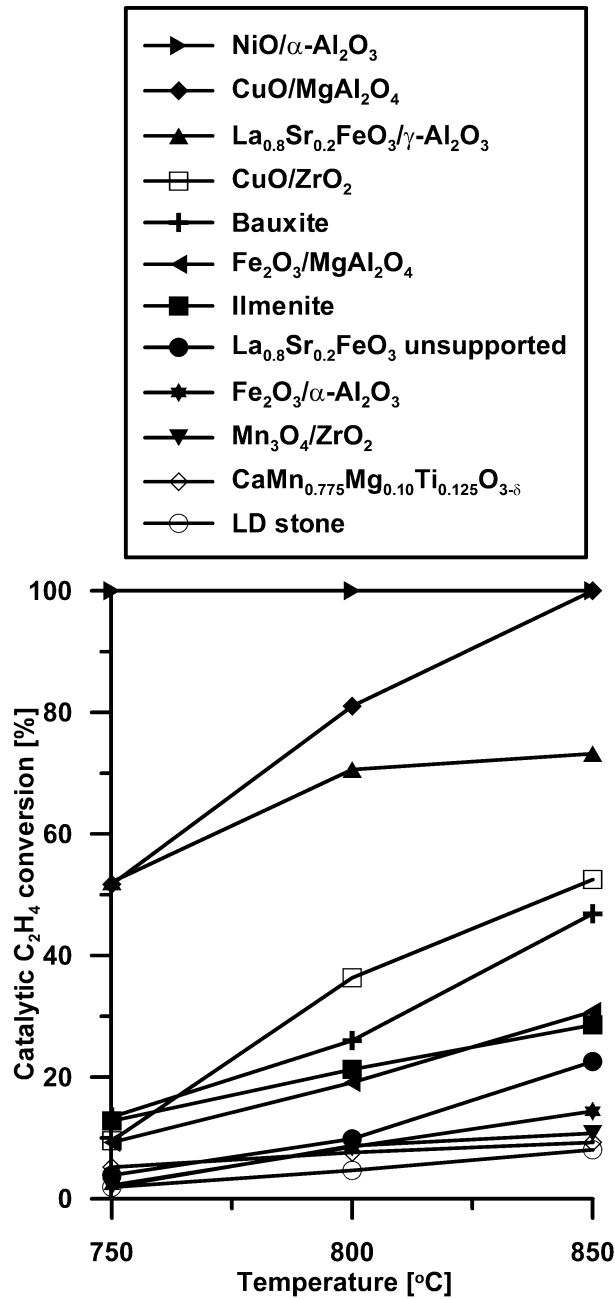**Table 4: Overview of bed materials used in the CLR screening study (Paper IV)**

Name	Composition	Production method	Ref.
$CaMn_{0.775}Mg_{0.10}Ti_{0.125}O_{3-\delta}$	100 wt% $CaMn_{0.775}Mg_{0.10}Ti_{0.125}O_{3-\delta}$	spray drying, calcined for 4h @ 1300°C	[95]
$CuO/MgAl_2O_4$	40 wt% CuO 60 wt% $MgAl_2O_4$ (Baikowski S30CR)	spray drying, calcined for 4h @ 1030°C	[96]
CuO/ZrO_2	40 wt% CuO 60 wt% ZrO_2	freeze granulation, calcined for 6h @ 1100°C	[97]
$Fe_2O_3/\alpha-Al_2O_3$	60 wt% Fe_2O_3 40 wt% $\alpha-Al_2O_3$ (Almatis CT3000SG)	freeze granulation, calcined for 6h @ 1100°C	[98]
$Fe_2O_3/MgAl_2O_4$	60 wt% Fe_2O_3 40 wt% $MgAl_2O_4$ (Baikowski S30CR)	freeze granulation, calcined for 6h @ 1100°C	[99]
$La_{0.8}Sr_{0.2}FeO_3$ unsupported	100 wt% $La_{0.8}Sr_{0.2}FeO_3$	spray drying, calcined for 10h @ 900°C	[100]
$La_{0.8}Sr_{0.2}FeO_3/\gamma-Al_2O_3$	10 wt%. $La_{0.8}Sr_{0.2}FeO_3$ 90 wt% $\gamma-Al_2O_3$ (Puralox NWa155)	impregnation, calcined for 2h @ 1100°C	-
Mn_3O_4/ZrO_2	37 wt% Mn_3O_4 63 wt% ZrO_2	freeze granulation, calcined for 6h @ 1100°C	[101]
$NiO/\alpha-Al_2O_3$	65 wt% NiO 35 wt% $\alpha-Al_2O_3$ (Almatis CT3000SG)	spray drying, calcined for 4h @ 1400°C	[102]
LD stone	LD slag is a waste product from steel-making process, provided by SS AB. Rich in Fe_2O_3, CaO, SiO_2 and MgO		
Bauxite	raw bauxite (Al_2O_3 and Fe_2O_3 mainly) calcined for 9h @ 850°C		
Ilmenite	activated rock ilmenite ($FeTiO_3$) provided by Titania A/S		
Quartz sand	used as reference		

In total, 13 different bed materials were screened for their utilization in CLR, out of which 4 are naturally occurring minerals/ores and 9 are synthesized particles. Quartz sand and a Ni-based material were used as reference materials. Materials were chosen so as to represent a range of fairly abundant and cheap transition metals such as Mn, Fe, and Cu. Most particles tested had previously been tested for utilization in CLC. References are provided in Table 4 which contain additional information on the particle synthesis and their properties. The elemental composition of the natural materials can be found in Table 3 in Paper IV. All of the synthetic particles consist of transition metal / metal oxides supported on different support materials, with the exception of the two unsupported, single-phase perovskitic materials $CaMn_{0.775}Mg_{0.10}Ti_{0.125}O_{3-\delta}$ and $La_{0.8}Sr_{0.2}FeO_3$.

In Figure 5 the catalytic C_2H_4 conversion as a function of reactor temperature for all screened bed materials is shown. The conversion is obtained during the experimental period when no oxygen is provided any longer by the bed material to the gas phase. For all tested materials the catalytic conversion increases with increasing reactor temperature. Unsurprisingly, the Ni-based material $NiO/\alpha-Al_2O_3$ achieves full C_2H_4 conversion at all temperatures. The Cu-based materials achieve a high degree of C_2H_4 conversion, with the conversion over $CuO/MgAl_2O_4$ being significantly higher than the conversion over CuO/ZrO_2. $La_{0.8}Sr_{0.2}FeO_3/\gamma-Al_2O_3$ also exhibits a high catalytic C_2H_4 conversion. Out of the natural bed materials investigated, bauxite exhibits the highest C_2H_4 conversion. Other Fe-based materials, such as the synthetic $Fe_2O_3/\alpha-Al_2O_3$, $Fe_2O_3/MgAl_2O_4$ and the unsupported $La_{0.8}Sr_{0.2}FeO_3$ as well as the natural mineral ilmenite possess a mediocre ability to convert C_2H_4 catalytically. The Mn-based materials Mn_3O_4/ZrO_2 and $CaMn_{0.775}Mg_{0.10}Ti_{0.125}O_{3-\delta}$ as well as LD stone exhibit a low catalytic C_2H_4 conversion.

Out of the investigated bed materials, only the Ni-containing bed material achieved full conversion of CH_4, whereas none of the other materials exhibited significant conversion of CH_4.

→ NiO/α-Al$_2$O$_3$

→ CuO/MgAl$_2$O$_4$

▲ La$_{0.8}$Sr$_{0.2}$FeO$_3$/γ-Al$_2$O$_3$

□ CuO/ZrO$_2$

+ Bauxite

◄ Fe$_2$O$_3$/MgAl$_2$O$_4$

■ Ilmenite

● La$_{0.8}$Sr$_{0.2}$FeO$_3$ unsupported

★ Fe$_2$O$_3$/α-Al$_2$O$_3$

▼ Mn$_3$O$_4$/ZrO$_2$

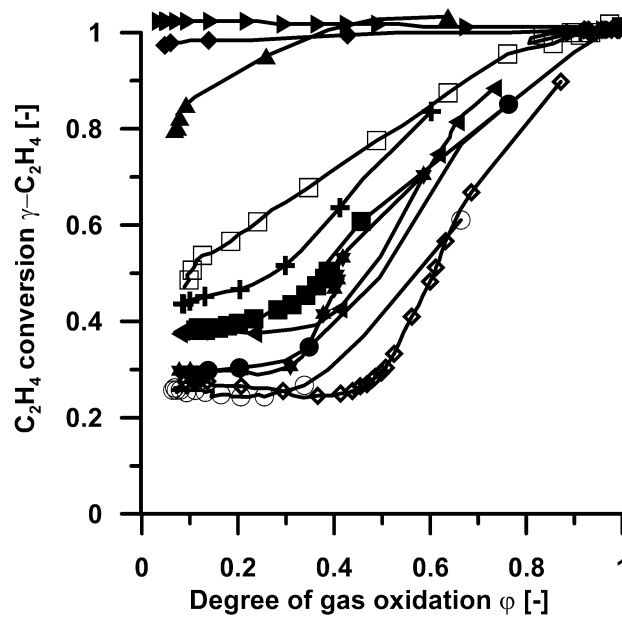◇ CaMn$_{0.775}$Mg$_{0.10}$Ti$_{0.125}$O$_{3-\delta}$

⊖ LD stone

Figure 5. Catalytic C$_2$H$_4$ conversion as a function of reactor temperature for all screened bed materials.

The catalytic conversion was determined when the gas conversion was stable and there was no transfer of oxygen from the particles, see Paper IV. However, upon initial exposure of the bed material to the gasification gas, there is an oxygen transfer from the bed material to the gas phase. Initially, the gasification gas is primarily oxidized to CO$_2$ and H$_2$O, but this is followed by a period of partial oxidation, which is of interest for CLR. In Figure 6 the total C$_2$H$_4$ conversion as a function of the degree of gas oxidation φ is shown for all screened bed materials. A φ of zero would indicate no oxygen transfer and only a catalytic conversion of the gasification gas compounds, whereas φ=1 would indicate full oxidation of the gasification

gas. In the figure, results are shown for T=800°C, with the total C_2H_4 conversion exhibiting similar trends at the two other investigated temperatures. It can be observed that $NiO/\alpha\text{-}Al_2O_3$ and $CuO/MgAl_2O_4$ achieve almost full C_2H_4 conversion independently of the degree of gas oxidation. In an ideal process, it is likely of interest to keep the oxidation of the gasification gas to a minimum in order to retain the heating value of the gas, and clearly both Ni- and the Cu- materials possess properties that allow this. Also, $La_{0.8}Sr_{0.2}FeO_3/\gamma\text{-}Al_2O_3$ and CuO/ZrO_2 exhibit an increase in C_2H_4 conversion already when rather small amounts of the gasification gas are oxidized by the material, which is an interesting property for their application in CLR. The other materials require a significant degree of gas oxidation of roughly 40% to increase the total C_2H_4 conversion. Operating a CLR unit under such conditions would result in a significant loss of cold gas efficiency of the gasification process.


Figure 6. Total C_2H_4 conversion as a function of the degree of gas oxidation φ at T=800°C for all screened bed materials (for legend, see Figure 5).

Another important criterion for the evaluation of bed materials for CLR is the oxygen transport capacity of the bed material. This can be expressed as the mass of oxygen per gram of bed material $\Delta\omega$ that is transported between the regenerator and the reformer. In Figure 7 $\Delta\omega$ is shown as a function of reactor temperature for all screened bed materials. The Cu-based particles, the Ni-based particles and $CaMn_{0.775}Mg_{0.10}Ti_{0.125}O_{3-\delta}$ particles possess a high oxygen transport capacity. The Fe-based bed materials and the Mn-based material exhibit a lower oxygen transport capacity. It should be noted that the percentage of metal oxide that can undergo reduction/oxidation reactions in CLR is different for each particle, which affects the comparison of the oxygen transport capacity of the different particles.
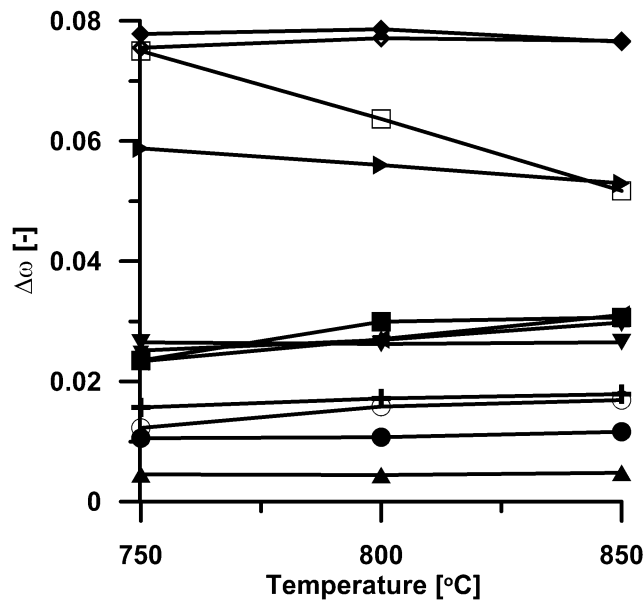
Figure 7. Mass of oxygen per gram of bed material transported by the bed material Δω as a function of reactor temperature for all screened bed materials (for legend, see Figure 5).

Finally, the amount of coke formation needs to be evaluated by measuring the gaseous carbon evolving from the bed material during its reoxidation. Figure 8 shows the coke formation as % of total C fed during 1000 seconds of exposure to gasification gas as a function of reactor temperature for all screened bed materials. It can be observed that only for the two Cu-based materials, $CuO/MgAl_2O_4$ and CuO/ZrO_2, a significant amount of carbon is deposited on the bed material, corresponding to a maximum of 4% of total added carbon at 850°C. On all other materials the amount of carbon deposited is comparably low. A more detailed study on the coke formation was conducted for $CuO/MgAl_2O_4$ and it was found that the onset of coke formation started when all CuO is reduced to elemental Cu. The amount of coke formation from then onwards increased linearly with exposure time.
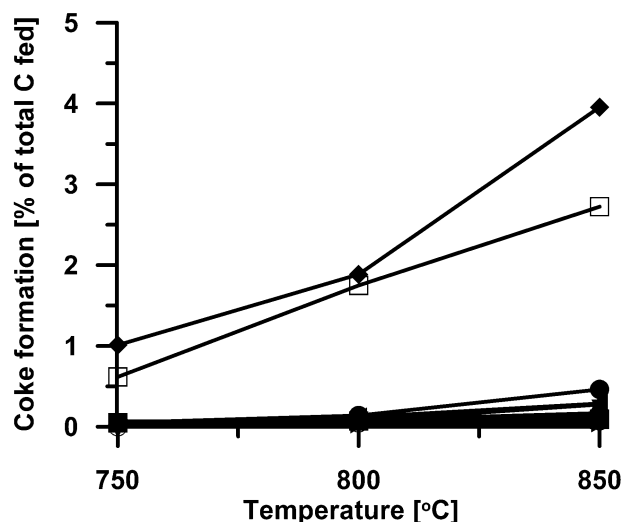
Figure 8. Coke formation as % of total C fed during 1000 seconds of exposure to gasification gas as a function of reactor temperature for all screened bed materials (for legend, see Figure 5).

It was further found that, out of all bed materials investigated, CuO/ZrO_2, unsupported $La_{0.8}Sr_{0.2}FeO_3$ and $Fe_2O_3/MgAl_2O_4$ experienced defluidization during operation. This demonstrates that the highly reducing conditions and high temperatures of the CLR reformer put stringent requirements on fluidizability of the bed materials; similar to those in the DFB process. For $La_{0.8}Sr_{0.2}FeO_3$, supporting the active phase on a substrate that does not undergo reduction, was found to be essential.

In summary, the screening study identified Cu-containing materials and supported $La_{0.8}Sr_{0.2}FeO_3$ materials as particularly promising bed materials for raw gasification gas conditioning in a CLR unit. Such materials were thus subjected for further tests. Cu-based materials are discussed in section 3.2 and La/Sr/Fe-based materials in section 3.3.

3.2. Cu-based active bed materials in CLR

Due to promising results obtained with Cu-containing supported materials such as spray-dried $CuO/MgAl_2O_4$ with ethylene, this material was subjected to further investigation. The reactivity of this material towards the monoaromatic compounds toluene and benzene included in the synthetic gasification gas feed was thus investigated (see Table 3 for gas compositions). Results of this investigation are described in more detail in Paper V appended to this thesis. In summary, it was found that $CuO/MgAl_2O_4$ was not able to convert monoaromatic compounds effectively. In fact, it was observed that the presence of aromatics inhibited the conversion of C_2H_4 drastically. The extent of this inhibition was found to depend on the partial pressure of monoaromatics in the feed gas. The large coke formation observed in the aromatics-free gas was not observed when monoaromatic compounds were present. This indicates that carbon formation is suppressed by the presence of monoaromatics. From the data obtained in this study, it can only be speculated what the mechanism of this suppression is. In previous research it was observed that, under similar experimental conditions, carbon is deposited on copper surfaces from mixtures of steam, H_2 and alkenes in the form of layered coke[103]. When comparing the adsorption energy on a Cu(111) surface of C_2H_4 (~0.13 eV)[104] with that of C_6H_6 (~0.6 eV)[105] one may assume that, in the presence of both C_6H_6 and C_2H_4, C_6H_6 adsorbs preferentially on the Cu surface and may form a monolayer or even graphene under the experimental conditions of this study. Cu is well known to be a potent catalyst for the formation of graphene[106]. Due to the presence of steam in the gas and therefore a rather high oxygen potential of the gas the formation of graphene oxide may even be plausible[107]. In any case, such a layer may then block the copper surface for the adsorption of C_2H_4 and thus inhibit the formation of coke from C_2H_4. The observation that C_2H_4 conversion decreases sharply with increasing C_6H_6 concentration in the feed further corroborates the existence of an inhibitory effect of monoaromatics on the coke formation from C_2H_4 on the Cu surface.

Cu-based materials were thus found to be unable to convert monoaromatic hydrocarbons catalytically, and may be of limited use if complete conversion of aromatics is desired in a gas conditioning process. However, they may still be of interest when a modified gas conditioning route is considered. As seen in Table 2 in section 3.1 the amount of BTX and its energy content in raw gas from DFB gasifier can be considerable. Instead of reforming BTX compounds, it might thus be economically attractive to recover them from the gas stream and sell them as byproducts of the SNG process as suggested by ECN[108]. In comparison to olefins and other light hydrocarbons, which would likely require separation by cryogenic distillation[109], BTX compounds could be separated with relative ease[110]. In that light, the selective conversion of olefins and the preservation of monoaromatic compounds in CLR with Cu-based bed materials appears promising. This would, however, require that the bed material

is able to convert olefins in the presence of aromatics. The spray-dried $CuO/MgAl_2O_4$ bed material does fall short because of the inhibition of olefins conversion by aromatics. It was thought that the strong inhibiting effect may arise from a limited active Cu surface area due to the use of micrometer-sized CuO powder as a precursor in the manufacture of this bed material. A further study was thus conducted in which a different production method and different support materials were investigated. The preparation of catalytically active bed materials by the impregnation of porous, Al_2O_3-based support material with aqueous solution of Cu salts could potentially generate materials with more favorable properties due to a higher dispersion of Cu. Four different Cu-impregnated support materials, both low-cost naturally occurring minerals and commercially available catalyst supports were thus investigated for their use in CLR.

The Cu content of the four impregnated materials was reduced from 40 wt-% CuO of the spray-dried $CuO/MgAl_2O_4$ to 10 wt-% CuO. The four porous support materials chosen were a commercial activated alumina catalyst support, an activated bauxite ore and two kaolinite-derived supports. In Table 5 their production parameters and the abbreviations that they are referred by are summarized. All impregnated materials were calcined at T=850°C for 20 hours in a muffle furnace in air. The purpose of this heat treatment was to decompose the metal nitrates and form the desired metal oxides as well as to account for initial changes in porosity/reactivity that are to be expected due to thermal sintering of the materials. Further details about the support materials can be found in Paper VI of this thesis.

Table 5. Overview over Cu-based bed materials produced by impregnation

	Support production precursors and method
Cu/PURALOX	commercial PURALOX NWa-155 γ-Al_2O_3 support
Cu/bauxite	high-gibbsite karst bauxite, activated at 650°C for 2 h
Cu/γ-Al_2O_3	kaolinite calcined at 1000°C for 24 h, then Si leached with NaOH
Cu/mullite	kaolinite calcined at 1100°C for 24 h, then Si leached with NaOH

In Figure 9 the conversion of C_2H_4, the conversion of C_6H_6 and the coke formation is shown as a function of the reactor temperature for the 4 different Cu-impregnated materials. Here, the inlet C_6H_6 volume fraction was 1.4%. It can be seen that none of the investigated materials could convert benzene effectively. With a high concentration of 1.4 % C_6H_6 in the feed, ethylene could only be effectively converted (over 80% conversion) when PURALOX was used as a support material. Cu/bauxite exhibited a degree of conversion somewhat higher than what could be observed with Cu/γ-Al_2O_3 and Cu/mullite. However, it is not a significant increase over the thermal conversion that was observed in the empty reactor experiment. As can be seen from Figure 9, only a small amount of the carbon contained in the gas is

deposited as coke on all of the bed materials. The highest coke formation is observed over Cu/bauxite at T=750°C. Over Cu supported on PURALOX, the amount of coke accounts for about 0.2% of the amount of carbon fed to the reactor. Together with the fact that up to 90% of the ethylene is converted by Cu/PURALOX and that no formation of larger hydrocarbons was observed, it can be concluded that ethylene is predominantly reformed into valuable syngas components CO and H_2.
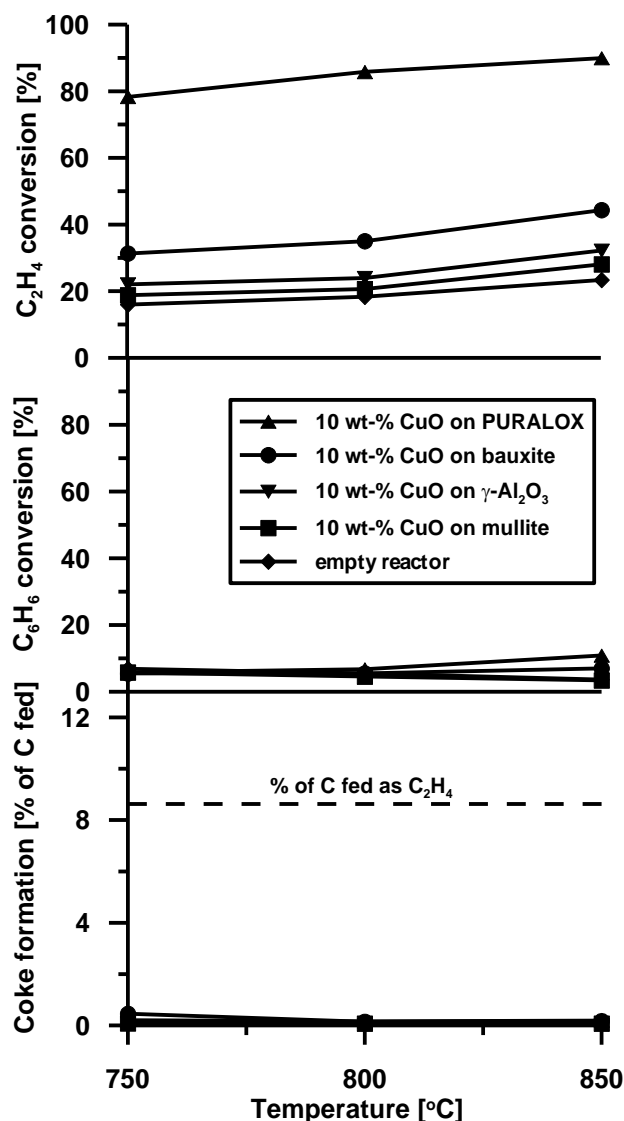
Figure 9. Catalytic conversion of C_2H_4, C_6H_6 and coke formation as a function of reactor temperature with 1.4 % C_6H_6 in the gas feed for four different Cu-impregnated materials and for an empty reactor experiment.

The behavior of the different materials during partial oxidation of the gasification gas was also investigated. It is shown in Figure 10 at T=800°C over Cu/mullite with 1.4 % C_6H_6 in the

gas feed as an example, with similar trends being observable for the other bed materials and temperatures. The conversion of C_2H_4 and C_6H_6 increases considerably with increasing degree of gas oxidation φ. The CH_4 conversion increases somewhat, but to a lesser extent, as indicated by the lower gradient. However, it needs to be observed that a significant portion of the gasification gas needs to be oxidized in order to achieve a substantial increase in C_2H_4 and C_6H_6 conversion.
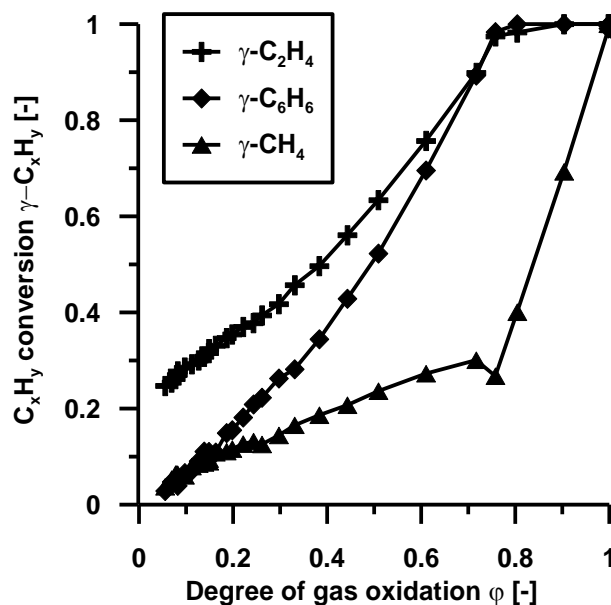

Figure 10. Hydrocarbon conversion as a function of degree of gas oxidation at T=800°C over Cu/mullite with 1.4 % C_6H_6 in the gas feed.

The oxygen transport property of the materials was also investigated. It was observed that for Cu/PURALOX, Cu/mullite and Cu/γ-Al_2O_3 the oxygen transport capacity was in good agreement with the theoretical value, corresponding to a complete reduction of Cu^{2+} to Cu^0, of about 2 wt-% of the mass of bed material. Cu/bauxite exhibited a somewhat higher oxygen transport due to the reducible iron oxide which this ore contains.

To investigate the inhibiting effect of monoaromatics on C_2H_4 conversion further, experiments with varying benzene inlet concentrations were conducted at T=800°C, the results of which are shown in Figure 11. For all 4 bed materials, an increase of C_2H_4 conversion was observed when the concentration of benzene was lowered, indicating an effective inhibition of ethylene conversion by the presence of benzene in the gas. This effect is very pronounced over Cu/bauxite, Cu/γ-Al_2O_3 and Cu/mullite, where the ethylene conversion decreased dramatically when benzene was present. For Cu/PURALOX, only a slight decrease of the ethylene conversion was observed with increasing benzene concentration, from full conversion at 0% C_6H_6 to about 90% conversion at 1.4% C_6H_6. With a decrease in benzene concentration, a drastic increase of coke formation was found for all investigated bed materials. If one

assumes that ethylene is the major source of carbon for the coke formation, it can be concluded that over Cu/mullite and Cu/bauxite, almost half of the fed ethylene was deposited as coke on the catalyst surface at low benzene concentrations of 0-0.2%. Over Cu/PURALOX, this effect is slightly less severe, with the coke formation peaking at about 40% of carbon fed as ethylene at a benzene concentration of 0.2%. From these observations, it can be concluded that over Cu/PURALOX the presence of high concentrations of benzene can prevent coke formation to some degree and thus stimulate the reforming of ethylene into syngas instead.
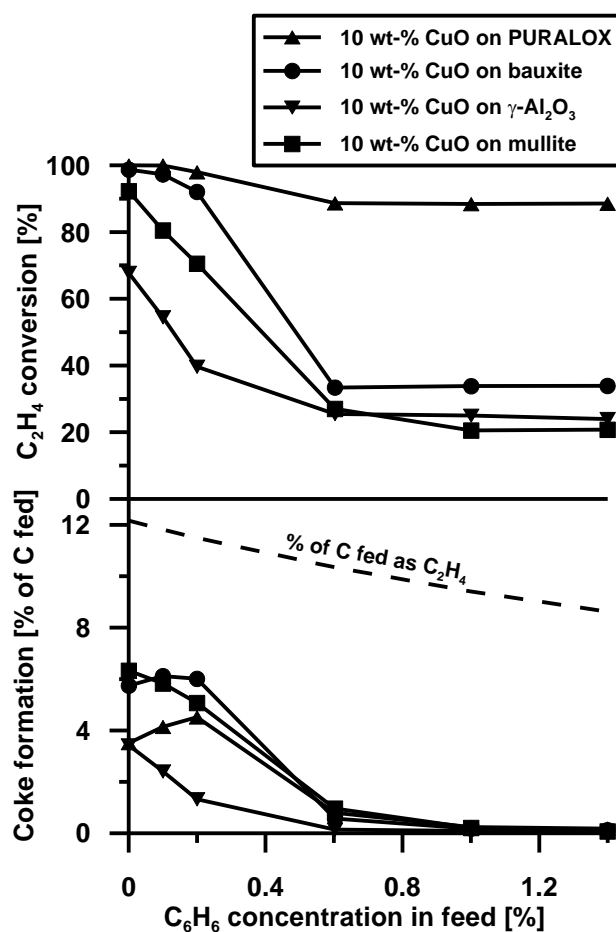
Figure 11. C_2H_4 conversion and coke formation at T=800°C as a function of C_6H_6 concentration in the gasification gas feed over Cu-impregnated bed materials.

Due to these encouraging results with Cu/PURALOX at T=800°C, further experiments were conducted with Cu/PURALOX to determine the conversion of ethylene at lower temperatures. Figure 12 shows the C_2H_4 conversion and coke formation as a function of C_6H_6 concentration in the gasification gas feed over Cu/PURALOX at T=600°C, T=700°C and T=800°C. At T=700°C the ethylene conversion and coke formation are slightly reduced, with the coke formation still being a strong function of C_6H_6 concentration in the feed. At T=600°C the ethylene conversion dropped to about 40%, while the coke formation was

reduced drastically even when no or little C_6H_6 was present. It might therefore be possible to convert ethylene effectively with little coke formation at T=600°C when the gas residence time is increased.
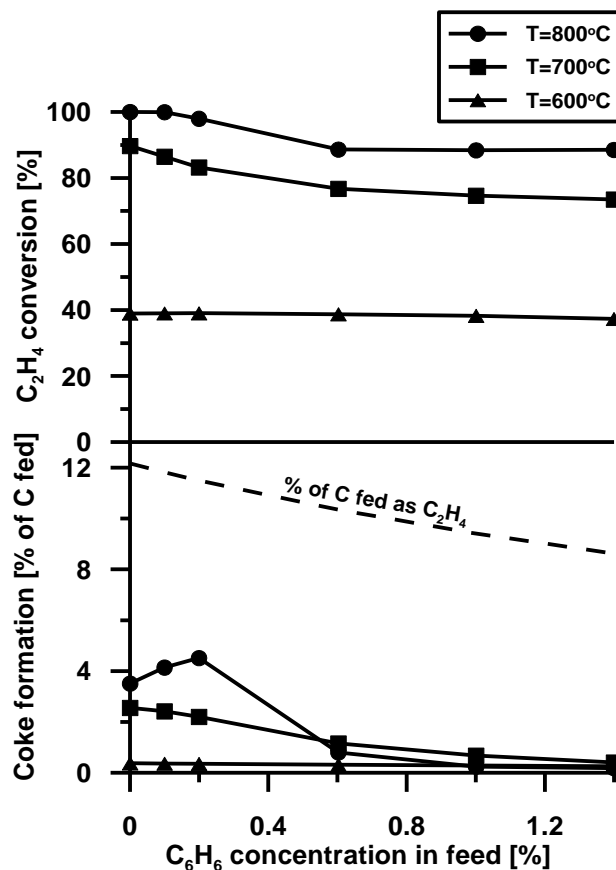
Figure 12. C_2H_4 conversion and coke formation as a function of C_6H_6 concentration in the gasification gas feed over Cu/PURALOX at T=600°C, T=700°C and T=800°C.

The behavior of Cu/PURALOX at T=600°C was thus investigated in more detail. In Figure 13 the gas concentration profiles as well as the extent of water gas shift reaction and the C_2H_4 conversion are shown as a function of exposure time of the bed material to gasification gas.
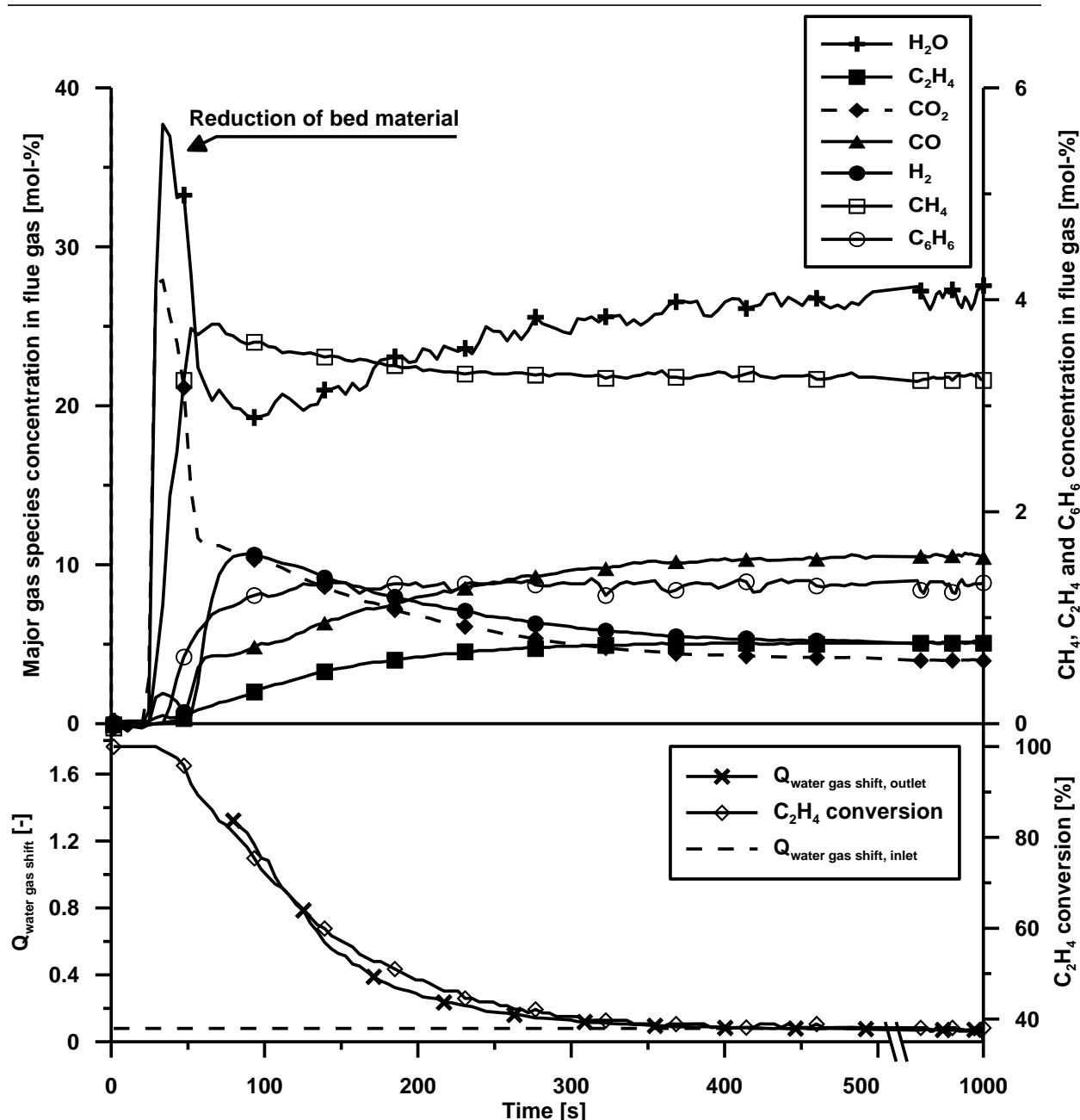
Figure 13. Recorded gas concentration profile (upper), extent of water gas shift reaction and C₂H₄ conversion (lower) during exposure to gasification gas with 1.4 % C₆H₆ in feed over Cu/PURALOX at T=600°C (Note that the x-axis is broken after the gas concentrations stabilize after 500 s).

After a short period of full combustion of the gas up to about t=40 s, the Cu^{2+} was reduced to Cu^0 and the bed material did not provide any oxygen to the gas any longer. At this point, the bed material was very active for the water gas shift reaction, indicated by the high $Q = \frac{[H_2][CO_2]}{[CO][H_2O]}$ ratio, the C₂H₄ conversion was very high and some additional CH₄ was generated. Over the course of the next 300 seconds, the activity of the bed material for the water gas shift

36

reaction, its conversion of C_2H_4 and its generation of CH_4 decreased simultaneously at the same rate. This suggests that in this period coke is formed via:

$$C_2H_4 \rightarrow CH_4 + C_{coke} \qquad (21)$$
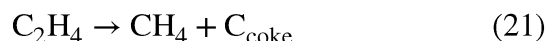
This is further corroborated by the observation that the amount of coke formed, the amount of CH_4 generated, and the amount of additional C_2H_4 converted during this coke formation period were approximately equimolar at 0.51-0.55 mmol. These findings indicate that in a CLR unit high ethylene conversion and a high extent of water gas shift could be achieved at temperatures as low as T=600°C when the amount of coke on the Cu/PURALOX surface is controlled carefully by recirculating the bed material fast enough. Furthermore, operating at a low temperature may also be beneficial when simultaneous H_2S removal is considered since the thermodynamics of sulfide formation are more favorable at lower temperatures[111,112].

Characterization of the bed material by N_2 adsorption and X-ray diffraction showed that all bed materials suffered from a decrease in pore volume when exposed to the gasification gas during the experiment. A more detailed analysis can be found in Paper VI. Although no decrease in reactivity of the bed materials was observed in the experiments, the long term stability of these porous materials needs to be investigated more in depth in future work.

In summary, it can be stated that all four Cu-containing materials produced by impregnating Al_2O_3-based support materials exhibited superior properties for their application in CLR compared to the spray-dried $CuO/MgAl_2O_4$. This indicates that dry impregnation of porous supports is a better suitable production method as compared to spray-drying for these CLR bed materials, likely due to the better dispersion of the active Cu phase. Nonetheless, all four investigated Cu-impregnated bed materials were prone to inhibition of ethylene conversion by the presence of monoaromatic compounds. However, for Cu impregnated on commercial PURALOX support, this inhibition was found to be rather weak.

Apart from the conversion of light hydrocarbons, in previous studies transition alumina based materials were also found to hold promise for the removal of heavy, polyaromatic tars from raw gasification gas[79,113]. This, however, has not been explicitly investigated in this work with Cu-impregnated transition alumina materials. The removal of heavy tars can significantly reduce the tar dew point and thus facilitate easier heat recovery from the gasification gas[114]. Cu-impregnated activated alumina could therefore be employed in a CLR unit to a) reform ethylene and other light hydrocarbons, b) potentially remove heavy tars from the gas stream, c) catalyze the water gas shift reaction and d) retain CH_4 and BTX compounds in it. BTX compounds could then be separated further downstream in the gas conditioning process.

3.3. La/Sr/Fe-containing supported active bed materials in CLR

3.3.1. La/Sr/Fe supported on Al_2O_3- and SiO_2-based support materials

From the initial screening study carried out in this work, it was observed that 10 wt-% $La_{0.8}Sr_{0.2}FeO_3$ supported on γ-Al_2O_3 exhibited high ethylene conversion and was thus deemed promising for its application in CLR gas conditioning. This material was therefore investigated further with benzene and toluene in the synthetic gasification gas. For reference, experiments were also conducted for the commercial activated γ-Al_2O_3 support material without $La_{0.8}Sr_{0.2}FeO_3$ and with an empty reactor. In Figure 14 the results of these three experiments are presented. The ethylene conversion over $La_{0.8}Sr_{0.2}FeO_3/\gamma$-$Al_2O_3$ was high even in the presence of benzene, and it was significantly higher than what was observed with only γ-Al_2O_3 support or the empty reactor. A rather high benzene conversion of almost 50% was achieved at T=850°C with $La_{0.8}Sr_{0.2}FeO_3/\gamma$-$Al_2O_3$, whereas no significant conversion could be seen with only γ-Al_2O_3 support or the empty reactor.
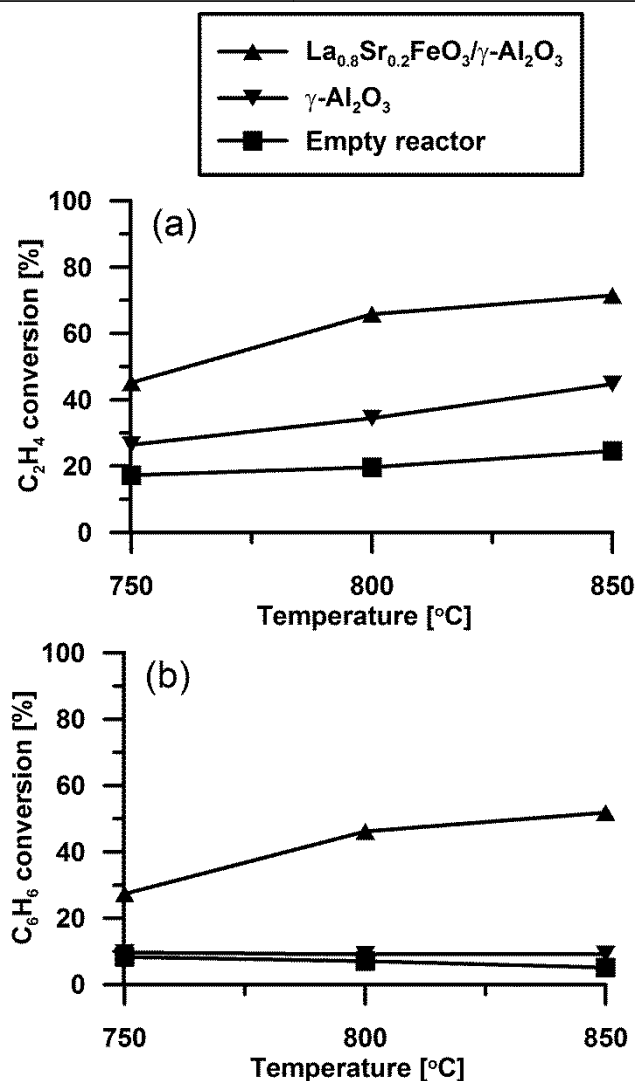
Figure 14. Conversion of (a) C_2H_4 and (b) C_6H_6 over $La_{0.8}Sr_{0.2}FeO_3/\gamma$-$Al_2O_3$ and γ-Al_2O_3 as a function of reactor temperature with 1.4% C_6H_6 in feed.

These results confirmed that the high reactivity is indeed exhibited by the $La_{0.8}Sr_{0.2}FeO_3$ phase, and not by the γ-Al_2O_3 support. This high activity for benzene reforming of the perovskite material initiated further research. Unsupported $La_{0.8}Sr_{0.2}FeO_3$ was omitted from further considerations because of its tendency to sinter under reducing conditions. The supported $La_{0.8}Sr_{0.2}FeO_3/\gamma$-$Al_2O_3$ material tested had been produced by impregnating micrometer-sized $La_{0.8}Sr_{0.2}FeO_3$ (LSFO) powder, pre-produced by wet chemical methods and ball milling, on the outside of larger γ-Al_2O_3 particles, leading to a rather small active $La_{0.8}Sr_{0.2}FeO_3$ surface area. After calcination at 1100°C, this synthesis approach results in a core-shell type structure with the active $La_{0.8}Sr_{0.2}FeO_3$ phase attached to the alumina support particles in the form of micrometer-sized grains. Two properties of the particles with this particular microstructure were deemed problematic:

1) When using such particles in fluidized beds, attrition would results in the loss of the active phase because it would affect mostly the outer shell of the active phase.

2) The active surface area of LSFO phase is limited due to its existence as micron-sized grains.

As a potential remedy for these issues, it was attempted to support the LSFO phase by impregnation of porous support materials, containing Al_2O_3, SiO_2 or mixtures thereof, in order to increase the active surface area of LSFO and to distribute the active phase more evenly throughout the particle. Porous support materials tested were wide-pore amorphous silica, commercial PURALOX γ-Al_2O_3, kaolinite-derived mullite and activated bauxite. However, after calcination at T=850°C, no LSFO perovskite phase was detectable with XRD analysis and none of the tested particles exhibited reactivity towards benzene when tested. When citric acid was added to the metal nitrate solution as a chelation agent, an LSFO phase was formed on some of the supports during calcination, but upon exposure to gasification gas it decomposed due to interaction with the Si and/or Al of the support. It was concluded that supporting LSFO on Al_2O_3- or SiO_2-containing substrates via the metal nitrate impregnation route is thus not feasible.

In order to at least alleviate the problem of the core-shell like structure of the original particles, it was then attempted to spray-dry 10 wt-% micrometer-sized LSFO powder with 90 wt-% Almatis CT3000sg α–Al_2O_3 of the same size range. Particles were calcined at 950, 1100 and 1150°C, and XRD analysis showed that the LSFO phase was still intact after calcination. However, none of these materials exhibited decent reactivity for benzene reforming during experimental tests. XRD analysis of the used particles retrieved from the reactor showed that the LSFO phase had indeed deteriorated. It can be speculated that this is due to the more intimate contact between the alumina support and the LSFO in the spray-dried particles as compared to the original core-shell type particles.

Due to these difficulties in supporting LSFO on SiO_2- and Al_2O_3-containing supports, it was instead attempted to support La/Sr/Fe on zirconia supports. This effort is reported on in section 3.3.2.

3.3.2. La/Sr/Fe supported on ZrO_2 support materials

ZrO_2 was investigated as a support material for La/Sr/Fe metals due to its relative chemical inertness, demonstrated by its use as a support for perovskites as a electrolyte material for solid oxide fuel cells[115], and its reported activity for selective catalytic oxidation of tars[116]. A more detailed account of this investigation is given in Papers VII and VIII of this thesis.

Bed materials were prepared via the incipient wetness method. Two different ZrO_2 support materials were investigated in order to determine the influence of the support microstructure

on benzene and ethylene conversion. One support material was a commercial, plasma processed monoclinic zirconia (Z-TECH LLC). This material provides porosity for impregnation since it exhibits a dendritic structure composed of zirconia crystals that are about 0.2 μm in size. This support material is abbreviated as ZTECH. The second support material was produced from zirconia nanopowder. This support material is abbreviated as ZNANO throughout this thesis. Further details information on the two support materials can be found in Paper VI.

ZTECH support material was impregnated with metal nitrates corresponding to 10 wt-% $La_{0.8}Sr_{0.2}FeO_3$ and 10 wt-% $LaFeO_3$. Furthermore, ZTECH was impregnated with individual La, Sr and Fe metal nitrates corresponding to the same molar amount of the corresponding metal that is included in the 10 wt-% $La_{0.8}Sr_{0.2}FeO_3$ materials. In Figure 15 the conversion of C_6H_6 and C_2H_4 is shown as a function of reactor temperature for these ZTECH impregnated materials and for an empty reactor experiment. It is evident from this data that the ZrO_2 support itself did not convert benzene. The impregnation with only Fe or Sr (ZTECH_Sr, ZTECH_Fe) yielded no significant benzene conversion either. ZTECH_La exhibited some marginal improvement of the benzene conversion at $T=850^\circ C$. However, only ZTECH_LaFe and ZTECH_LaSrFe exhibited significant and rather high degrees of benzene conversion. When comparing ZTECH_LaFe and ZTECH_LaSrFe it can be seen that the addition of Sr greatly improves the benzene conversion. Similar trends that were observed for the benzene conversion could be seen for the ethylene conversion, with the exception that ZTECH_Fe exhibits a significantly higher conversion than the unimpregnated support and ZTECH_Sr.
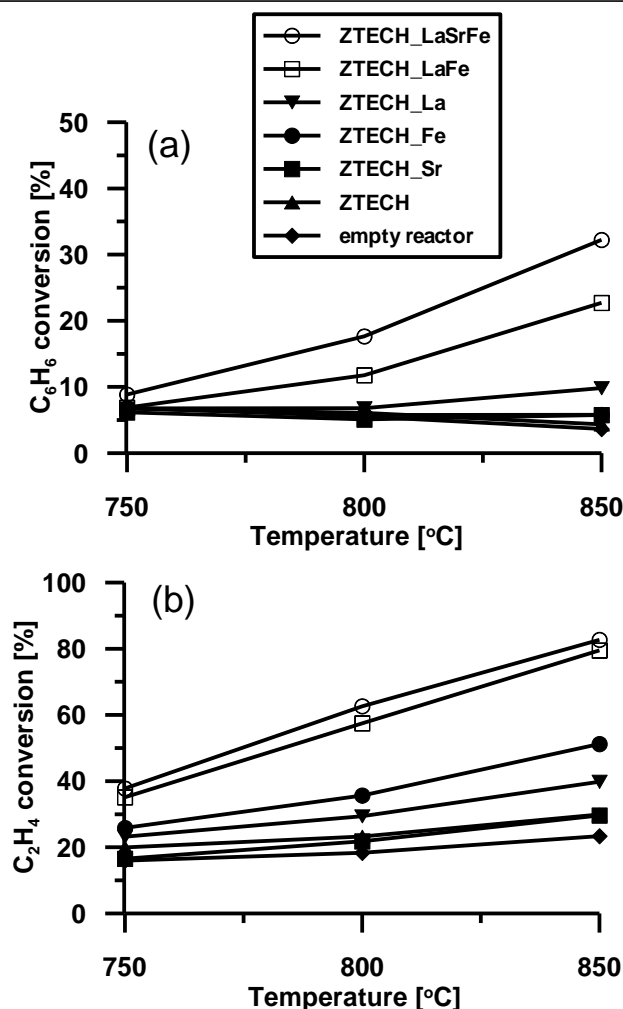
Figure 15. Conversion of (a) C_6H_6 and (b) C_2H_4 as a function of reactor temperature with 1.4 % C_6H_6 in the gas feed for the different ZTECH ZrO_2 impregnated materials and for an empty reactor experiment.

To investigate the influence of support microstructure on conversion, metal nitrates corresponding to 10 wt-% $La_{0.8}Sr_{0.2}FeO_3$ were impregnated on the other investigated support material ZNANO as well. Analysis of the impregnated materials by N_2 adsorption showed that ZNANO-based material exhibited a porous structure after impregnation and calcination with pores of about 30-100 nm in size. This porous structure was, however, destroyed during the experiment. The tapped bulk density of used ZNANO_LaSrFe was determined to be 1.02 g/ml, whereas the tapped bulk density of used ZTECH_LaSrFe was 2.48 g/ml and thus significantly higher. From this difference in density and the low pore volume of ZNANO_LaSrFe determined by N_2 adsorption, it can be concluded that the ZNANO_LaSrFe contains significant pore volume in the form of macropores > 200 nm that cannot be resolved by N_2 adsorption measurements, even more so than the ZTECH_LaSrFe material. This macroporous structure was confirmed by SEM investigation of the ZNANO particles.

In Figure 16 the benzene conversion and the ethylene conversion over these two materials is compared. It can be seen that in a mass-based comparison ZNANO_LaSrFe achieved a significantly higher degree of both benzene and ethylene conversion. It is conceivable that this is due to a longer gas residence time in the fluidized bed as a result of a higher macroporosity and thus a lower bulk density of the ZNANO_LaSrFe particles.
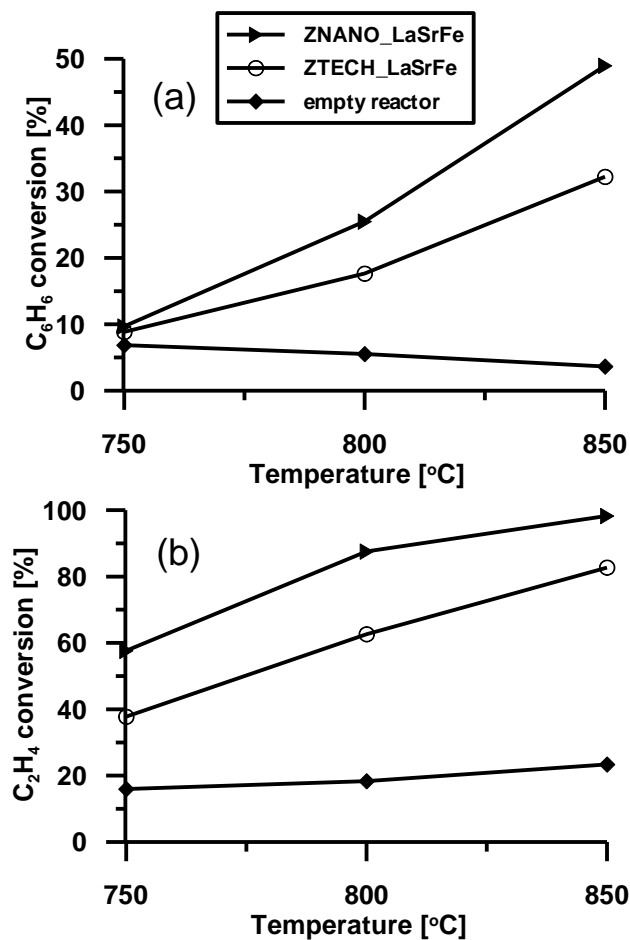

Figure 16. Conversion of (a) C_6H_6 and (b) C_2H_4 as a function of reactor temperature with 1.4 % C_6H_6 in the gas feed for ZTECH_LaSrFe, ZNANO_LaSrFe and for an empty reactor experiment.

XRD analysis of ZTECH_LaSrFe was conducted at the following stages: before the experiment, after the experiment when quenched in N_2 gas after the exposure to gasification gas at 800°C, and after that material had been reoxidized in air at 800°C for 1h. After calcination, only monoclinic ZrO_2, a $ZrSiO_4$ impurity and perovskitic $La_{0.8}Sr_{0.2}FeO_3$ phases could be observed. During the experiment the $La_{0.8}Sr_{0.2}FeO_3$ perovskite phase decomposed and reacted with the ZrO_2 support to form $La_2Zr_2O_7$ pyrochlore and minor quantities of $SrZrO_3$ perovskite. Even after reoxidation at 800°C in air, the $La_{0.8}Sr_{0.2}FeO_3$ perovskite phase could not be restored, and the pyrochlore phase remained.

The combined results of the reactivity tests and the XRD analysis thus indicate that on the La/Sr/Fe-impregnated ZrO_2 materials, the perovskite phase is not the active phase responsible for the high reactivity. Instead, the catalytic activity may be caused by the formation of a doped $La_2Zr_2O_7$ phase. In that case, the impregnation with La/Sr/Fe ratios corresponding to an LSFO perovskite phase may not necessarily be ideal. Therefore, in a next step, the influence of Sr/La-ratio and Fe/La ratio on the activity and properties of these materials was investigated. For that purpose ZNANO support was impregnated with a constant molar amount of La, 3 different Sr/La ratios at a constant Fe/La ratio of 1.25 (corresponding to the original LSFO composition), and 6 different Fe/La ratios at a constant Sr/La ratio of 0.25. An overview of these synthesized materials can be found in Table 2 in Paper VIII. The influence of Sr/La on C_6H_6 and C_2H_4 conversion is shown in Figure 17. At Sr/La=0, the reactivity towards C_6H_6 is lower than at the original Sr/La=0.25. When the Sr loading is doubled to Sr/La=0.5, the reactivity was found to decrease slightly. It was concluded that an increase in Sr loading does not result in a higher reactivity, and as a consequence, Sr/La was fixed to 0.25 for further experiments.
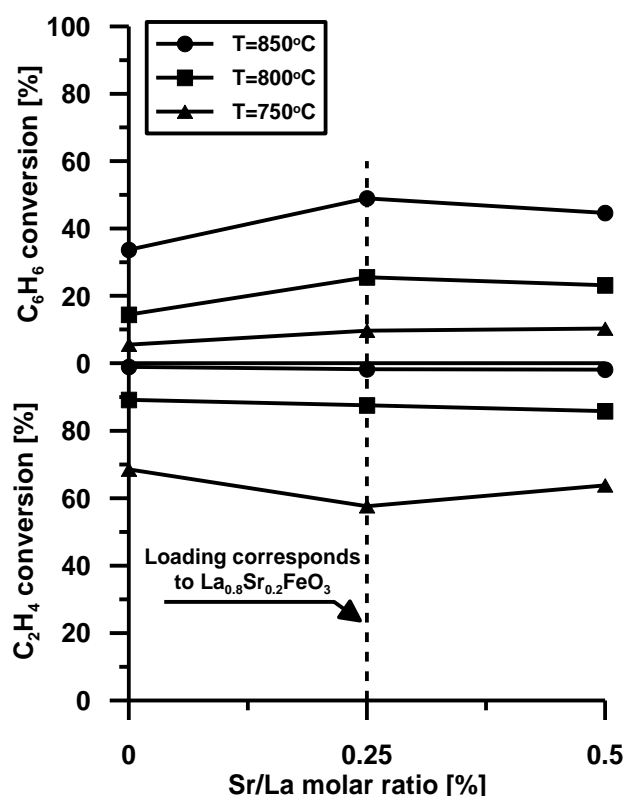
Figure 17. Conversion of C_6H_6 and C_2H_4 as a function of Sr/La molar ratio of ZNANO supported materials with Fe/La=1.25 at three different temperatures with 1.4 % C_6H_6 in the gas feed.

In Figure 18 the influence of the Fe/La ratio on the reactivity at Sr/La=0.25 is shown. A higher loading of Fe than the original loading corresponding to the perovskite composition

resulted in a decrease of reactivity for steam reforming of C_6H_6. When the Fe loading is decreased compared to this value, the reactivity towards C_6H_6 increases significantly, up to about 60% conversion at T=850°C at Fe/La=0.25, and then decreases drastically at Fe/La<0.25. Simultaneously, the reactivity towards C_2H_4 decreases when the Fe loading is decreased over the complete range of loadings investigated.

This decrease of reactivity with decrease in Fe loading is to be expected when considering the results shown in Figure 15, where it is shown that Fe impregnated on its own on ZrO_2 already exhibited a significant reactivity towards C_2H_4, but not towards C_6H_6. In any case, at Fe/La=0.25 the C_2H_4 conversion is still considerably higher than the C_6H_6 conversion, indicating that this ratio is ideal when complete conversion of C_2H_4 and C_6H_6 is the objective.
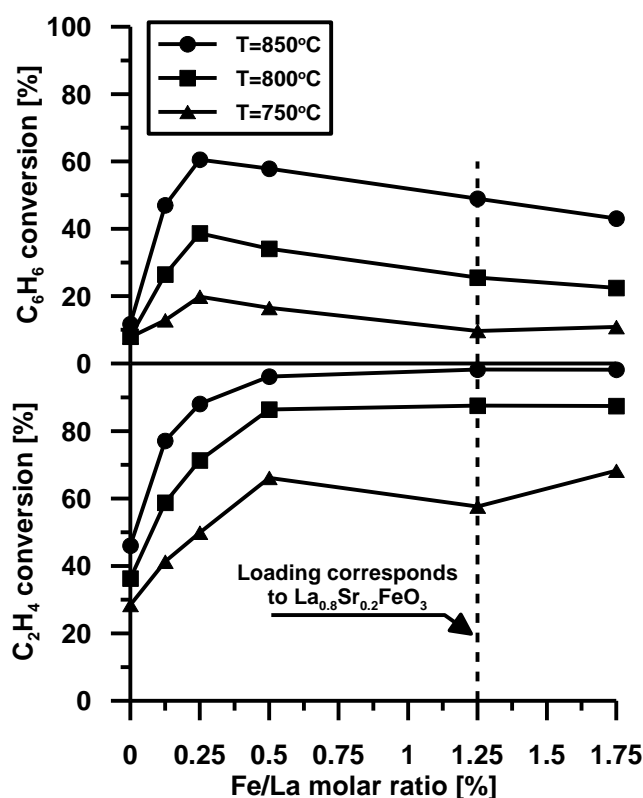

Figure 18. Conversion of C_6H_6 and C_2H_4 as a function of Fe/La molar ratio of ZNANO supported materials with Sr/La=0.25 at three different temperatures with 1.4 % C_6H_6 in the gas feed.

At a loading of Fe/La=0.25 and Sr/La=0.25, the total loading of metals onto the ZrO_2 support material is considerably lower at 0.57 mmol/g support as compared to 0.96 mmol/g support of the original material. This simplifies the impregnation procedure because at such low loadings, double impregnation with intermediate drying is not required anymore. In an attempt to further increase the conversion of benzene and ethylene, the support material was impregnated with twice the molar amount of metals (1.14 mmol/ g support total loading) with the optimized composition Fe/La=0.25 and Sr/La=0.25. The reactivity of this material as

compared to the material with half the loading is shown in Figure 19. It was found that a doubling in total loading did not result in any increase in reactivity towards benzene. The reactivity towards ethylene increased somewhat, but not by much.
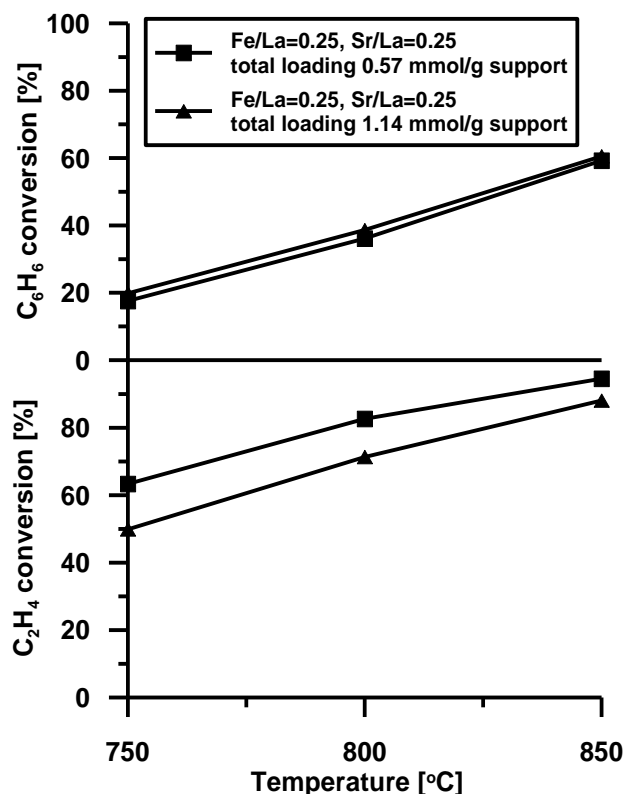
Figure 19. Conversion of C_6H_6 and C_2H_4 as a function of temperature of ZNANO supported materials with Fe/La=0.25, Sr/La=0.25 at total metal loadings of 0.57 mmol/g support and 1.14 mmol/ g support with 1.4 % C_6H_6 in the gas feed.

XRD analysis of the used materials (for details see Paper VIII) showed that $La_2Zr_2O_7$ pyrochlore was always formed during the experiments in all samples, and $SrZrO_3$ was formed when Sr was present in the sample. At the highest investigated Fe loading of Fe/La=1.75 a separate FeO phase was formed, whereas at all other Fe loading, no Fe oxide phase could be detected. Fe and, to a lower extent, Sr are likely soluble in the pyrochlore phase, as discussed in more detail in Paper VIII. The average crystallite size of the pyrochlore phase was found to be as low as 14 nm. This, together with the result of the SEM/EDS analysis that showed that La, Fe and Sr are well distributed on the surface already at Fe/La=0.25, could indicate that the pyrochlore phase was well dispersed on the ZrO_2 support surface. In turn, this good dispersion, observed already at a low total loading, could then serve as an explanation as to why no significant increase in catalytic activity when doubling the total impregnated metal loading could be observed. It could thus be concluded that at the total loading of 0.57 mmol/g

support, the surface coverage of the active phase was already sufficiently high to maximize reactivity.

Apparent kinetic data obtained for these materials indicate that the steam reforming reaction of benzene is approximately first order with respect to the benzene concentration. Apparent reaction rate constants can then be obtained when plug flow and a negligible gas expansion are assumed.

$$k = -\frac{\ln\left(1-\frac{\gamma_{C_6H_6}}{100}\right)}{\tau} \tag{22}$$

Here, $\gamma_{C_6H_6}$ denotes the conversion of benzene and τ denotes the gas residence time that can be approximated via the bulk density of the bed material, the mass of the bed material and the volumetric flow rate in the reactor.

$$\tau = \frac{m_{\text{bed material}}}{\varrho_{\text{bulk,bed material}} \, V} \tag{23}$$

The conversion of benzene can then be predicted as a function of the Gas Hourly Space Velocity based on bulk bed volume GHSV, defined as:

$$GHSV = \frac{T_N}{T} \frac{1}{\tau} \tag{24}$$

The prediction of benzene conversion over ZNANO with Fe/La=0.25 and the improvement of conversion over the original composition with Fe/La=1.25 as a function of GHSV is shown in Figure 20. Especially at lower temperatures of 750°C and 800°C the predicted improvement of benzene conversion by decreasing the Fe loading is considerable.
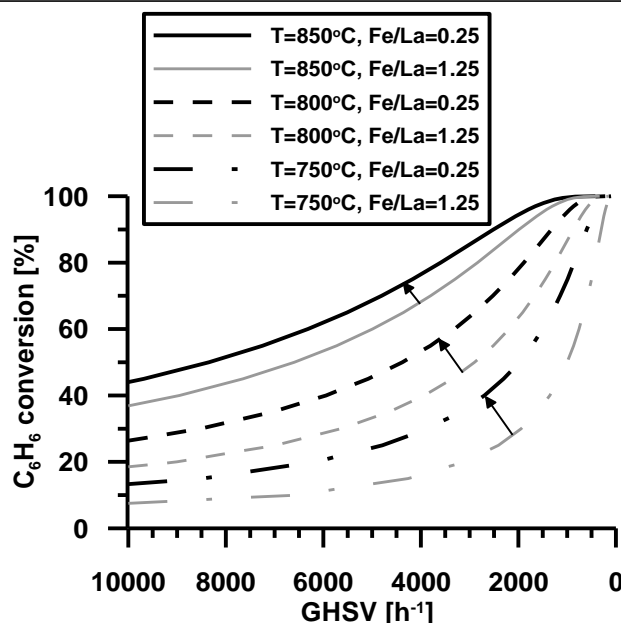
Figure 20. Prediction of benzene conversion over ZNANO with Fe/La=0.25 and Fe/La=1.25 as a function of Gas Hourly Space Velocity (GHSV) for three different temperatures, using simple kinetic model.

In addition to the catalytic conversion of hydrocarbons during the period when no oxygen transport is occurring any longer, the partial oxidation behavior of ZrO_2-supported materials was determined. Due to the low amount of oxygen transported by these materials as a consequence of the fairly low loading with reducible Fe species, the period of partial oxidation was short. For the material with a higher Fe loading of Fe/La=1.25, the periods of full and partial oxidation of the gas were prolonged by conducting experiments with only 25% wet gasification gas in N_2. By lowering the reactant concentration it was thus possible to discern actual partial oxidation from transient effects in the measurement system. The conversion of hydrocarbons during this partial oxidation period over ZNANO with Fe/La=1.25 and Sr/La=0.25 at T=800°C is shown in Figure 21. It was observed that the C_2H_4 conversion and the CH_4 conversion did not increase during the partial oxidation of the gas by the bed material. In contrast, the conversion of benzene was significantly increased already at small values of φ when only a limited amount of oxygen was provided by the bed material.
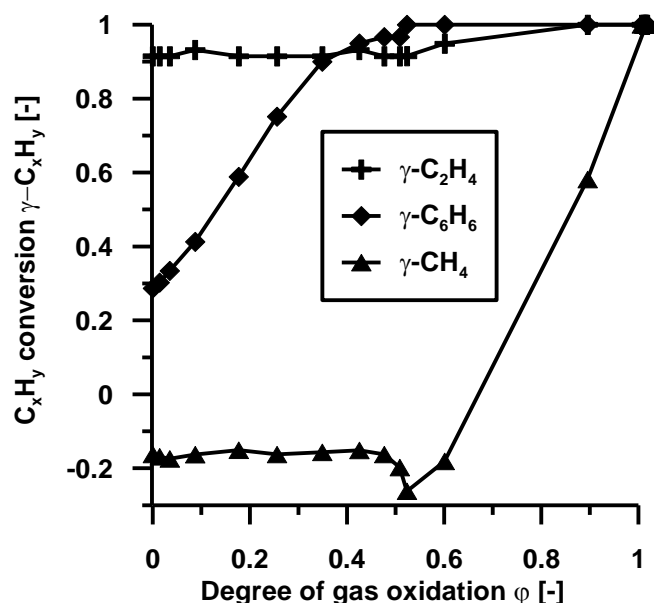
Figure 21. Hydrocarbon conversion as a function of degree of gas oxidation at T=800°C over ZNANO with Fe/La=1.25 and Sr/La=0.25 with 25% wet gasification gas mixture and 75% N₂ in the feed. The negative conversion values for methane indicate formation of CH₄.

For the material with a reduced Fe loading of Fe/La=0.25 that was found to be ideal with respect to benzene conversion, a reliable determination of transient behavior was no longer possible. This was due to the limited oxygen transport and thus a too short oxidation period. Its activity for Selective Catalytic Oxidation was instead investigated by adding molecular oxygen to the inlet gasification gas. Concentrations of 0, 1 and 2 % of O_2 in the feed gas were investigated and, at the same time, the C_6H_6 inlet concentration was varied between 0.6, 1, 1.4 and 1.8 % at T=750-850°C (see Figure 22). The addition of O_2 increased C_6H_6 conversion at all temperatures and all C_6H_6 inlet concentration, however not very drastically. To illustrate, an increase in reaction temperature by 50°C leads to larger increase in conversion than the addition of 2 % O_2 to the inlet gas, which corresponds to 8 % O_2 on dry gasification gas basis. The dependence of benzene conversion on the C_6H_6 inlet concentration with no oxygen in feed was rather weak, indicating that the steam reforming reaction of benzene is of first order with respect to the benzene concentration.
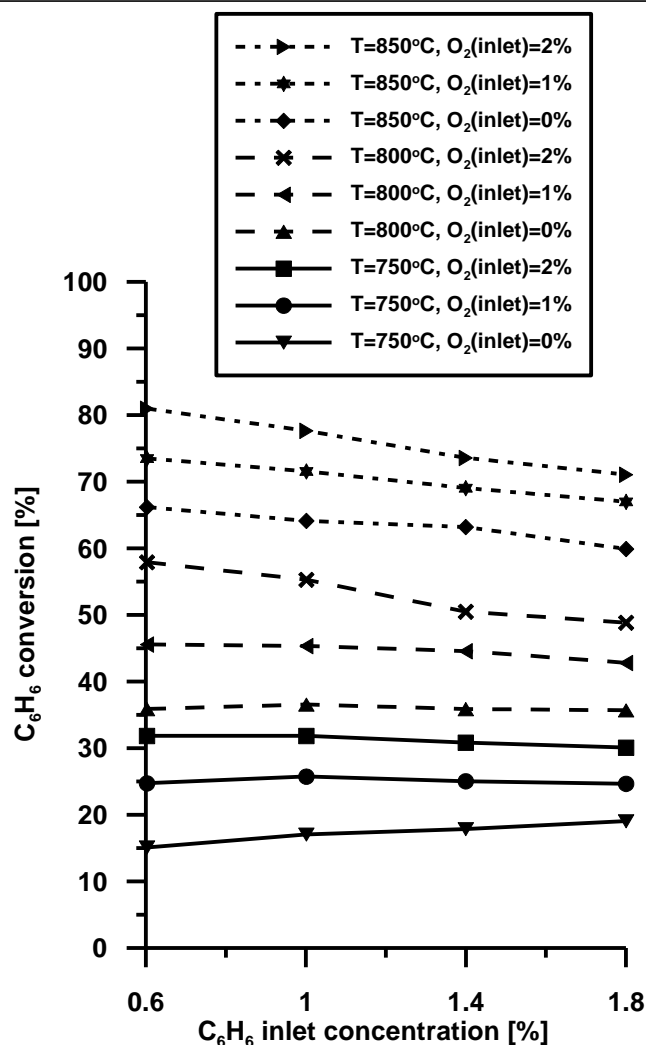
Figure 22. Benzene conversion as a function of benzene inlet concentration at three different temperatures of 750°C, 800°C and 850°C and O_2 inlet concentrations of 0, 1 and 2 mol-% over ZNANO with Fe/La=0.25 and Sr/La=0.25.

When oxygen is added to the feed, there is a dependence of the C_6H_6 conversion on the inlet C_6H_6 concentration. This can be visualized by plotting the increase in C_6H_6 conversion in percentage points with O_2 in the feed as compared to no O_2 in the feed, as shown in Figure 23. The increase of benzene conversion with decreasing benzene inlet concentration is more pronounced at 2 % O_2 in the feed as compared to 1 % O_2 in the feed, but still rather weak.

Ethylene conversion was improved by the addition of O_2 to the gasification gas, but to a lesser extent than benzene. In contrast to benzene and ethylene, methane was not converted by the added oxygen.

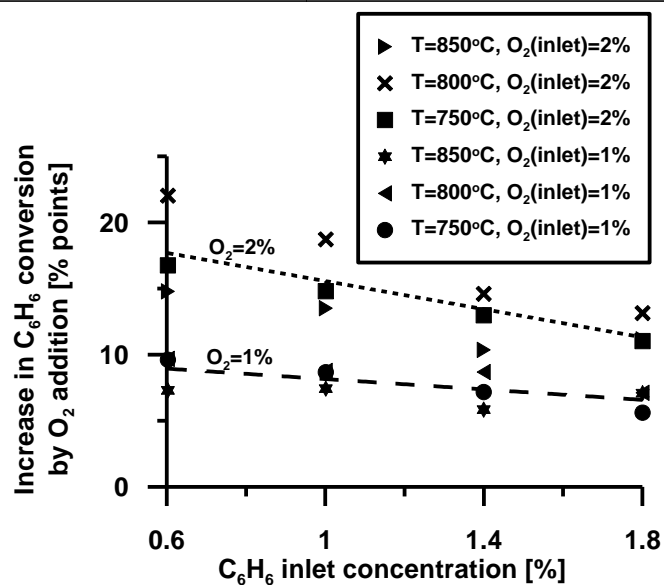**Figure 23.** Increase in benzene conversion as a function of benzene inlet concentration at three different temperatures of 750°C, 800°C and 850°C and O_2 inlet concentrations of 1 and 2 mol-% over ZNANO with Fe/La=0.25 and Sr/La=0.25.

4. Discussion

In this thesis some novel metal oxide have been investigated as bed materials in dual fluidized beds systems for gasification or gas conditioning. It was shown that, when gasifying char in the presence of metal oxide bed materials in a fluidized bed, the char gasification rate can be increased considerably. This could be attributed to the decrease in hydrogen inhibition by effective removal of hydrogen by its oxidation by the metal oxide bed material. As a consequence, remarkably higher char gasification rates can be realized in a CLC fuel reactor than in steam gasification processes without reducible metal oxide bed materials present. Exploitation of such an effect has also been attempted in a DFB gasifier with 12 wt-% ilmenite mixed with sand as active bed material[44]. However, no significant increase in char conversion was observed. Instead, a substantial amount of the product gas was combusted, resulting in a lower cold-gas efficiency[44]. These results indicate that decreasing hydrogen inhibition with active metal oxides may not be a viable measure for increasing the gasification rate in a DFB gasifier, and may instead best be exploited in the context of CLC.

An alternative way of increasing char gasification rate is by introducing potent gasification catalysts with the active bed material. In this work the in-situ transport of Potassium as catalyst from a Manganese ore bed material to the fuel was demonstrated for the first time. A subsequent investigation of various other manganese ores revealed that the char gasification rate increases with the content of potassium and sodium in the ores, indicating catalytic steam gasification as the dominant char conversion mechanism in the presence of these ores[117]. Recently, a number of publications investigated the use of Potassium-impregnated iron-based bed materials for CLC, both natural iron ores and synthetic bed materials[118–124]. Such impregnation, however, requires the treatment of the bed material before usage, which would likely induce additional costs. In this light, catalyzing the gasification reaction by catalysts already included in cheap natural ores which can be utilized as bed materials appears economically more attractive. This is because neither an impregnation of the large solid fuel mass stream nor an impregnation of the bed material are required as additional processing steps. The utilization of such a material thus seems very promising. However, as alkali components are known to cause problems with respect to corrosion, this aspect also needs to be further investigated for a possible future application of Potassium-bearing bed materials in CLC or gasification processes.

The utilization of metal oxide bed materials in raw gasification gas conditioning via a dual-fluidized bed CLR process was also investigated in this work. A comprehensive screening of first-row transition metal oxide-containing bed materials was conducted. The propensity to convert ethylene varied considerably depending upon the bed material. It was shown that ethylene could be converted both catalytically and through partial oxidation to various

degrees using these materials. Based on this screening investigation, several new and promising materials were developed and investigated in detail. Two especially promising bed materials were developed, namely Cu-impregnated activated alumina and Fe,Sr-doped $La_2Zr_2O_7$ supported on ZrO_2. The major properties of interest for their application in CLR gas conditioning are summarized in Table 6.

Table 6. Comparison of properties of interest for CLR of two promising bed materials

	Reactivity towards C_2H_4	Reactivity towards C_6H_6	Oxygen transport capacity	Coke formation
Cu / PURALOX	high	low	high	high
Fe,Sr-doped $La_2Zr_2O_7$ / ZrO_2	high	high	low	low

Cu-containing bed materials were found to exhibit high degrees of ethylene conversion, but did not convert BTX compounds at an appreciable rate. They are therefore attractive for use in gas conditioning process configurations where the objective is to separate BTX from the gas stream and market them as byproducts. Fe,Sr-doped lanthanum zirconates exhibited high degrees of conversion of both ethylene and monoaromatics, and are thus attractive when the reforming of all hydrocarbons, except methane, is desired. However, the latter materials contain only a very small quantity of Fe that would be able to transport oxygen via redox reactions. Furthermore, these ZrO_2-supported materials were quite resistant to coke formation and thus, only little heat can be generated by the combustion of coke in the regenerator. The steam reforming of hydrocarbons that is catalyzed on the particle surface is endothermic in nature. As a consequence, partial oxidation of some of the syngas is thus required to maintain operating temperature of the CLR unit. When catalysts with such a low oxygen transport capacity are used in CLR, oxygen for partial oxidation could alternatively be provided by mixing these catalysts with bed materials with a higher oxygen transport capacity. To exploit Selective Catalytic Oxidation properties of such Fe,Sr-doped $La_2Zr_2O_7$ / ZrO_2 catalysts, it might be further advantageous to utilize bed materials that can release gaseous oxygen in the reformer as oxygen transport materials. In the last 15 years a large number of oxygen carrier materials have been developed, both materials which can oxidize fuels directly and also materials which can release oxygen to the gas phase[16]. It is expected that there are such oxygen carriers available which would be viable to combine with the Fe,Sr-doped $La_2Zr_2O_7$ / ZrO_2 catalysts. For instance, the Cu/PURALOX bed material developed in this work may be an alternative, as it has a high oxygen carrying capacity and may possess a gaseous oxygen release property at temperatures relevant for CLR[125]. This may thus be a promising way of

achieving a high degree of conversion of ethylene and monoaromatics and partially oxidize the raw gasification gas effectively.

Generally, the prospect of employing active bed materials in the processes illustrated in Figure 1, does not solely depend on their reactivity or other favorable properties from a reaction engineering point-of-view, but also on cost considerations. Substantial costs can arise from using these bed materials, associated with the cost of raw materials and, for synthetic materials, also with costs for the production of the bed materials. When the bed material is directly mixed with solid fuels in the primary loop of a gasification system, the lifetime would likely be limited due to deactivation or removal with the ash. For a CLR system downstream of the gasifier, longer bed material lifetimes could be expected, and thus higher bed material costs may be acceptable. An attempt at illustrating how bed material cost and bed material lifetime are connected is appended to this thesis.

5. Conclusions

In this work metal oxide bed materials for efficient solid fuel gasification and gas clean-up in fluidized beds have been investigated. In the primary loop of a DFB gasifier or a CLC fuel reactor, employing such active bed materials can be an effective measure to increase the char gasification rate. It was shown that such an increase in gasification rate can be the result of 1) a decrease in hydrogen inhibition by efficient removal of hydrogen from the vicinity of the gasifying char particle, or of 2) the transfer of a catalyst via the bed material to the char, which in turn catalyzes the steam-carbon gasification reaction.

Metal oxide bed materials can also be utilized downstream of the primary gasifier loop in a dual-fluidized bed CLR process. Here, the main purpose of such a system is to condition the raw gasification gas by reforming tars and hydrocarbons. In this work, in total more than 45 metal oxide based materials were developed and/or investigated for application in the CLR process. Two promising groups of metal oxide bed materials were identified: 1) Cu-impregnated alumina and 2) Fe,Sr-doped lanthanum zirconates.

All investigated Cu-impregnated bed materials exhibited only minor reactivity towards benzene. Further, the presence of monoaromatics effectively inhibited the conversion of ethylene on these materials. However, for Cu impregnated on commercial activated alumina PURALOX support, this inhibition was found to be rather weak, and up to 90% ethylene conversion was obtained at T=850°C.

Fe,Sr-doped lanthanum zirconates achieved high degrees of ethylene and benzene conversion via steam reforming. With these materials the benzene and ethylene conversion could be further increased by co-feeding O_2 with the gasification gas. With 2 mol-% O_2 in the feed a benzene conversion of 80% and an ethylene conversion of about 95% at T=850°C and at a high Gas Hourly Space Velocity of 6800 h^{-1} was achieved.

6. References

1. McKendry P. Energy production from biomass (part 3): Gasification technologies. Bioresour Technol. 2002;83(1):55-63.

2. Chmielniak T, Sciazko M. Co-gasification of biomass and coal for methanol synthesis. Appl Energy. 2003;74(3-4):393-403.

3. Bridgwater a V. The technical and economic feasibility of biomass gasification for power generation. Fuel. 1995;74(5):631-653.

4. Minchener AJ. Coal gasification for advanced power generation. Fuel. 2005;84(17):2222-2235.

5. Higman C, Van Der Burgt MJ. Gasification (Second Edition).; 2007.

6. Higman C, Tam S. Advances in Coal Gasification, Hydrogenation, and Gas Treating for the Production of Chemicals and Fuels. Chem Rev. 2014;114:1673-1708.

7. Hayashi JI, Kudo S, Kim HS, Norinaga K, Matsuoka K, Hosokai S. Low-temperature gasification of biomass and lignite: Consideration of key thermochemical phenomena, rearrangement of reactions, and reactor configuration. Energy and Fuels. 2014;28(1):4-21.

8. Jüntgen H. Application of catalysts to coal gasification processes. Incentives and perspectives. Fuel. 1983;62(2):234-238.

9. Panthi D, Choi B, Tsutsumi A. A Novel Type of Micro-Tubular SOFC for Application in Super IGFC System. In: *Proceedings of the AIChE 2012 Spring Meeting and 8th Global Congress on Process Safety 2012*. Vol ; 2012.

10. Karl J. Biomass heat pipe reformer—design and performance of an indirectly heated steam gasifier. Biomass Convers Biorefinery. 2013;4(1):1-14.

11. Schuster G, Löffler G, Weigl K, Hofbauer H. Biomass steam gasification--an extensive parametric modeling study. Bioresour Technol. 2001;77(1):71-79.

12. Kawabata M, Kurata O, Iki N, Tsutsumi A, Furutani H. System modeling of exergy recuperated IGCC system with pre- and post-combustion CO2 capture. Appl Therm Eng. 2013;54(1):310-318.

13. Kawabata M, Kurata O. Advanced integrated gasification combined cycle (A-IGCC) by exergy recuperation--technical challenges for future generations. J Power Technol. 2012;92(2):90-100.

14. Matsuoka K, Hosokai S, Kato Y, et al. Promoting gas production by controlling the interaction of volatiles with char during coal gasification in a circulating fluidized bed gasification reactor. Fuel Process Technol. 2013;116:308-316.

15. Lyngfelt A. Oxygen Carriers for Chemical Looping Combustion - 4 000 h of Operational Experience. Oil Gas Sci Technol – Rev d'IFP Energies Nouv. 2011;66(2):161-172.

16. Adanez J, Abad A, Garcia-Labiano F, Gayan P, de Diego LF. Progress in Chemical-Looping Combustion and Reforming technologies. Prog Energy Combust Sci. 2012;38(2):215-282.

17. Borah RC, Ghosh P, Rao PG. A review on devolatilization of coal in fluidized bed. Int J Energy Res. 2011;35(April):929-963.

18. Vassilev S V., Baxter D, Andersen LK, Vassileva CG. An overview of the chemical composition of biomass. Fuel. 2010;89(5):913-933.

19. Roberts DG, Harris DJ. Char gasification in mixtures of CO_2 and H_2O: Competition and inhibition. Fuel. 2007;86(17-18):2672-2678.

20. Lussier MG, Zhang Z, Miller DJ. Characterizing rate inhibition in steam/hydrogen gasification via analysis of adsorbed hydrogen. Carbon N Y. 1998;36(9):1361-1369.

21. Hüttinger KJ, Merdes WF. The carbon-steam reaction at elevated pressure: Formations of product gases and hydrogen inhibitions. Carbon N Y. 1992;30(6):883-894.

22. Giberson RC, Walker JP. Reaction of Nuclear Graphite with Water Vapor Part I. Effect of Hydrogen and Water Vapor Partial Pressures. Carbon N Y. 1966;3:521-525.

23. Bayarsaikhan B, Sonoyama N, Hosokai S, et al. Inhibition of steam gasification of char by volatiles in a fluidized bed under continuous feeding of a brown coal. Fuel. 2006;85(3):340-349.

24. Weeda M, Abcouwer HH, Kapteijn F, Moulijn JA. Steam gasification kinetics and burn-off behaviour for a bituminous coal derived char in the presence of H2. Fuel Process Technol. 1993;36(1-3):235-242.

25. Mims CA. Catalytic gasification of carbon: fundamentals and mecbanism. In: *Fundamental Issues in Control of Carbon Gasification Reactivity.* Vol ; 1991:383-407.

26. Nishiyama Y. Catalytic gasification of coals - Features and possibilities. Fuel Process Technol. 1991;29:31-42.

27. Moulijn JA, Kapteijn F. Towards a unified theory of reactions of carbon with oxygen-containing molecules. Carbon N Y. 1995;33(8):1155-1165.

28. Nahas NC. Exxon catalytic coal gasification process - Fundamentals to flowsheets. Fuel. 1983;62:239-241.

29. McKee DW, Chatterji D. The catalyzed reaction of graphite with water vapor. Carbon N Y. 1978;16(1):53-57.

30. Mims C, Pabst J. Alkali-catalyzed carbon gasification kinetics: Unification of H2O, D2O, and CO2 reactivities. J Catal. 1987;107(1):209-220.

31. Meijer R, Kapteijn F, Moulijn J. Kinetics of the alkali-carbonate catalysed gasification of carbon: 3. H2O gasification. Fuel. 1994;73(5):723-730.

32. Martinez-Alonso A, Tascon JMD. The Determining Role of Mineral Matter on Gasification Reactivities of Brown Coal Chars. In: *Fundamental Issues in Control of Carbon Gasification Reactivity.* Vol ; 1991:435-460.

33. Olsson J, Larsson J, Sette E, Pallarès D, Sasic S, Johnsson F. Experimental Evaluation of the Lateral Mixing of Fuel in a Fluidized Bed with Cross-Flow of Solids – Influence of Tube Banks. In: *11th International Conference on Fluidized Bed Technology, CFB 2014.* Vol ; 2014:119-124.

34. Kramp M, Thon a., Hartge E-U, Heinrich S, Werther J. Carbon Stripping - A Critical Process Step in Chemical Looping Combustion of Solid Fuels. Chem Eng Technol. 2012;35(3):497-507.

35. Cao Y, Pan W. Investigation of Chemical Looping Combustion by Solid Fuels. 1. Process Analysis. Energy & Fuels. 2006;(20):1836-1844.

36. Dong L, Asadullah M, Zhang S, Wang XS, Wu H, Li CZ. An advanced biomass gasification technology with integrated catalytic hot gas cleaning Part I. Technology and initial experimental results in a lab-scale facility. Fuel. 2013;108:409-416.

37. Ahrenfeldt J, Henriksen U, Jensen TK, et al. Validation of a continuous combined heat and power (CHP) operation of a two-stage biomass gasifier. Energy and Fuels. 2006;20(6):2672-2680.

38. Wang J, Sakanishi K, Saito I, Takarada T, Morishita K. High-yield hydrogen production by steam gasification of HyperCoal (ash-free coal extract) with potassium carbonate: Comparison with raw coal. Energy and Fuels. 2005;19(5):2114-2120.

39. Zhang S, Min Z, Tay H-L, Asadullah M, Li C-Z. Effects of volatile–char interactions on the evolution of char structure during the gasification of Victorian brown coal in steam. Fuel. 2011;90(4):1529-1535.

40. Li CZ. Importance of volatile-char interactions during the pyrolysis and gasification of low-rank fuels - A review. Fuel. 2013;112:609-623.

41. Matsuoka K, Hosokai S, Kuramoto K, Suzuki Y. Enhancement of coal char gasification using a pyrolyzer–gasifier isolated circulating fluidized bed gasification system. Fuel Process Technol. 2013;109:43-48.

42. Guan G, Fushimi C, Tsutsumi A, et al. High-density circulating fluidized bed gasifier for advanced IGCC/IGFC—Advantages and challenges. Particuology. 2010;8(6):602-606.

43. Masaki K, Kashimura N, Takanohashi T, Sato S, Matsumura A, Saito I. Effect of pretreatment with carbonic acid on "HyperCoal" (ash-free coal) production from low-rank coals. Energy and Fuels. 2005;19(5):2021-2025.

44. Larsson A, Israelsson M, Lind F, Seemann M, Thunman H. Using ilmenite to reduce the tar yield in a dual fluidized bed gasification system. Energy and Fuels. 2014;28(4):2632-2644.

45. Linderholm C, Lyngfelt A, Cuadrat A, Jerndal E. Chemical-looping combustion of solid fuels – Operation in a 10kW unit with two fuels, above-bed and in-bed fuel feed and two oxygen carriers, manganese ore and ilmenite. Fuel. 2012;102:808-822.

46.   Arjmand M, Leion H, Lyngfelt A, Mattisson T. Use of manganese ore in chemical-looping combustion (CLC)—Effect on steam gasification. Int J Greenh Gas Control. 2012;8:56-60.

47.   Frohn P, Arjmand M, Azimi G, Leion H, Mattisson T, Lyngfelt A. On the High-Gasification Rate of Brazilian Manganese Ore in Chemical-Looping Combustion (CLC) for Solid Fuels. AIChE J. 2013;59(11):4346-4354.

48.   Zhang Y, Hara S, Kajitani S, Ashizawa M. Modeling of catalytic gasification kinetics of coal char and carbon. Fuel. 2010;89(1):152-157.

49.   Lind F, Israelsson M, Seemann M, Thunman H. Manganese oxide as catalyst for tar cleaning of biomass-derived gas. Biomass Convers Biorefinery. 2012;2(2):133-140.

50.   Van der Meijden CM, van der Drift A, Vreugdenhil BJ. Experimental results from the allothermal biomass gasifier Milena. In: *15th European Biomass Conference.* Vol ; 2008.

51.   Schmid JC, Wolfesberger U, Koppatz S, Pfeifer C, Hofbauer H. Variation of Feedstock in a Dual Fluidized Bed Steam Gasifier — Influence on Product Gas , Tar Content , and Composition. Environ Prog Sustain Energy. 2012;31(2):205-215.

52.   Baumhakl C, Karl J, Kienberger T, et al. Substitute Natural Gas from Coal with Internal Sequestration of CO2 (CO2freeSNG).; 2013.

53.   Grootjes AJ, Aranda G, Van Der Meijden CM, Van Der Drift A, Vreugdenhil BJ. I-MILENA Gasification Technology for (high Ash) Low Rank Coal.; 2014.

54.   Li C, Suzuki K. Tar property, analysis, reforming mechanism and model for biomass gasification—An overview. Renew Sustain Energy Rev. 2009;13(3):594-604.

55.   Bartholomew C. Mechanism of catalyst deactivation. Appl Catal A Gen. 2001;212:17-60.

56.   Cui H, Turn SQ, Keffer V, Evans D, Tran T, Foley M. Contaminant estimates and removal in product gas from biomass steam gasification. Energy and Fuels. 2010;24(2):1222-1233.

57.   Kaufman Rechulski MD, Schildhauer TJ, Biollaz SMA, Ludwig C. Sulfur containing organic compounds in the raw producer gas of wood and grass gasification. Fuel. 2014;128:330-339.

58.   Torres W, Pansare SS, Goodwin JG. Hot Gas Removal of Tars, Ammonia, and Hydrogen Sulfide from Biomass Gasification Gas. Catal Rev. 2007;49(4):407-456.

59.   Swisher JH, Schwerdtfeger K. Review of Metals and Binary Oxides as Sorbents for Removing Sulfur from Coal-Derived Gases. J Mater Eng Perform. 1992;1(June):399-407.

60.   Cheah S, Carpenter DL, Magrini-Bair K a. Review of mid- to high-temperature sulfur sorbents for desulfurization of biomass- and coal-derived syngas. Energy and Fuels. 2009;23(November 1998):5291-5307.

61.   Denton D, Gardner B, Gupta R, Turk B. Pre-commercial demonstration of high efficiency, low cost syngas cleanup technology for chemical, fuel, and power applications. In: *31st Annual International Pittsburgh Coal Conference: Coal - Energy, Environment and Sustainable Development, PCC 2014.* Vol ; 2014.

62.   Cheah S, Olstad JL, Jablonski WS, Magrini-Bair KA. Regenerable Manganese-Based Sorbent for Cleanup of Simulated Biomass-Derived Syngas. Energy and Fuels. 2011;25(1):379-387.

63.   Cheah S, Parent YO, Jablonski WS, Vinzant T, Olstad JL. Manganese and ceria sorbents for high temperature sulfur removal from biomass-derived syngas - The impact of steam on capacity and sorption mode. Fuel. 2012;97:612-620.

64.   König CFJ, Nachtegaal M, Seemann M, et al. Mechanistic studies of chemical looping desulfurization of Mn-based oxides using in situ X-ray absorption spectroscopy. Appl Energy. 2014;113:1895-1901.

65.   Devi L, Ptasinski KJ, Janssen FJJG. A review of the primary measures for tar elimination in biomass gasification processes. Biomass and Bioenergy. 2002;24:125-140.

66.   Pecho J, Schildhauer TJ, Sturzenegger M, Biollaz S, Wokaun a. Reactive bed materials for improved biomass gasification in a circulating fluidised bed reactor. Chem Eng Sci. 2008;63(9):2465-2476.

67.   Corella J, Aznar MP, Delgado J, Martinez MP, Aragües JL. The Deactivation of Tar Cracking Stones (Dolomites, Calcites, Magnesites) and of Commercial Methane Steam Reforming Catalysts in the Upgrading of the Exit Gas from Steam Fluidized Bed Gasifiers of Biomass and Organic Wastes. Stud Surf Sci Catal. 1991;68:249-252.

68.   Bain RL, Dayton DC, Carpenter DL, et al. Evaluation of Catalyst Deactivation during Catalytic Steam Reforming of Biomass-Derived Syngas. Ind Eng Chem Res. 2005;44(21):7945-7956.

69.   Lind F, Seemann M, Thunman H. Continuous Catalytic Tar Reforming of Biomass Derived Raw Gas with Simultaneous Catalyst Regeneration. Ind Eng Chem Res. 2011;50(20):11553-11562.

70.   Dayton D, Kataria A, Gupta R. Biomass Gas Cleanup Using a Therminator.; 2012.

71.   Abu El-Rub Z, Bramer E a., Brem G. Review of Catalysts for Tar Elimination in Biomass Gasification Processes. Ind Eng Chem Res. 2004;43(22):6911-6919.

72.   Orìo A, Corella J, Narvàez I. Performance of Different Dolomites on Hot Raw Gas Cleaning from Biomass Gasification with Air. Ind Eng Chem Res. 1997;36:3800-3808.

73.   Devi L, Ptasinski KJ, Janssen FJJG, Van Paasen SVB, Bergman PC a, Kiel JH a. Catalytic decomposition of biomass tars: Use of dolomite and untreated olivine. Renew Energy. 2005;30:565-587.

74.   Simell PA, Hirvensalo EK, Smolander VT. Steam Reforming of Gasification Gas Tar over Dolomite with Benzene as a Model Compound. Ind Eng Chem Res. 1999;38:1250-1257.

75.   Delgado J, Aznar P, Corella J. Calcined dolomite, magnesite, and calcite for cleaning hot gas from a fluidized bed biomass gasifier with steam: life and usefulness. Ind Eng Chem Res. 1996;35:3637-3643.

76.   Gusta E, Dalai AK, Uddin MA, Sasaoka E. Catalytic decomposition of biomass tars with dolomites. Energy and Fuels. 2009;23(4):2264-2272.

77.   Simell PA, Hakala NAK, Haario HE. Catalytic decomposition of gasification gas tar with benzene as the model compound. Ind Eng Chem Res. 1997;36:42-51.

78.   Simell PA, Leppälahti JK, Bredenberg JB. Catalytic purification of tarry fuel gas with carbonate rocks and ferrous materials. Fuel. 1992;71:211-218.

79.   Simell PA, Bredenberg JB -so. Catalytic purification of tarry fuel gas. Fuel. 1990;69(10):1219-1225.

80.   Simell PA, Leppälahti JK, Bredenberg JB. Catalytic purification of tarry fuel gas with carbonate rocks and ferrous materials. Fuel. 1992;71(2):211-218.

81.   Abu El-Rub Z, Bramer E a., Brem G. Experimental comparison of biomass chars with other catalysts for tar reduction. Fuel. 2008;87(10-11):2243-2252.

82.   Shen Y. Chars as carbonaceous adsorbents/catalysts for tar elimination during biomass pyrolysis or gasification. Renew Sustain Energy Rev. 2015;43:281-295.

83.   Hosokai S, Kumabe K, Ohshita M, Norinaga K, Li CZ, Hayashi JI. Mechanism of decomposition of aromatics over charcoal and necessary condition for maintaining its activity. Fuel. 2008;87(13-14):2914-2922.

84.   Buchireddy PR, Bricka RM, Rodriguez J, Holmes W. Biomass Gasification: Catalytic Removal of Tars over Zeolites and Nickel Supported Zeolites. Energy and Fuels. 2010;24(4):2707-2715.

85.   Woltermann GM, Magee JS, Griffith SD. Commercial Preparation and Characterization of FCC Catalysts. Stud Surf Sci Catal. 1993;76:105-144.

86.   Jones G, Jakobsen J, Shim S, et al. First principles calculations and experimental insight into methane steam reforming over transition metal catalysts. J Catal. 2008;259(1):147-160.

87.   Rönkkönen H, Simell P, Reinikainen M, Niemelä M, Krause O. Precious metal catalysts in the clean-up of biomass gasification gas Part 1: Monometallic catalysts and their impact on gasification gas composition. Fuel Process Technol. 2011;92(8):1457-1465.

88.   Rönkkönen H, Simell P, Niemelä M, Krause O. Precious metal catalysts in the clean-up of biomass gasification gas part 2: Performance and sulfur tolerance of rhodium based catalysts. Fuel Process Technol. 2011;92(10):1881-1889.

89. Rönkkönen H, Simell P, Reinikainen M, Krause O, Niemelä MV. Catalytic clean-up of gasification gas with precious metal catalysts - A novel catalytic reformer development. Fuel. 2010;89(11):3272-3277.

90. Mei D, Lebarbier VM, Rousseau R, et al. Comparative Investigation of Benzene Steam Reforming over Spinel Supported Rh and Ir Catalysts. ACS Catal. 2013;3(6):1133-1143.

91. Steele AM, Poulston S, Magrini-Bair K, Jablonski W. Catalytic syngas purification from model biomass gasification streams. Catal Today. 2013;214:74-81.

92. Lind F, Berguerand N, Seemann M, Thunman H. Ilmenite and nickel as catalysts for upgrading of raw gas derived from biomass gasification. Energy and Fuels. 2013;27:997-1007.

93. Marinkovic J, Berguerand N, Lind F, Seemann M, Thunman H. Using a manganese ore as catalyst for upgrading biomass derived gas. Biomass Convers Biorefinery. 2015;5:75-83.

94. Berguerand N, Lind F, Israelsson M, Seemann M, Biollaz S, Thunman H. Use of Nickel Oxide as a Catalyst for Tar Elimination in a Chemical-Looping Reforming Reactor Operated with Biomass Producer Gas. Ind Eng Chem Res. 2012;51(51):16610-16616.

95. Arjmand M, Kooiman RF, Ryden M, Leion H, Mattisson T, Lyngfelt A. Sulphur Tolerance of CaxMn1−yMyO3−d (M = Mg, Ti) Perovskite-type Oxygen Carriers in Chemical-Looping with Oxygen Uncoupling (CLOU). Energy & Fuels. 2014;28(2):1312-1324.

96. Adánez-Rubio I, Arjmand M, Leion H. Investigation of combined supports for Cu-based oxygen carriers for chemical-looping with oxygen uncoupling (CLOU). Energy and Fuels. 2013;27:3918-3927.

97. Johansson M. Screening of Oxygen-Carrier Particles Based on Iron-, Manganese-, Copper-and Nickel Oxides for Use in Chemical-Looping Technologies.; 2007.

98. Mattisson T, Johansson M, Lyngfelt A. Multicycle reduction and oxidation of different types of iron oxide particles application to chemical-looping combustion. Energy & Fuels. 2004:628-637.

99. Johansson M, Mattisson T, Lyngfelt A. Investigation of Fe2O3 with MgAl2O4 for chemical-looping combustion. Ind Eng Chem Res. 2004;43(i):6978-6987.

100. Rydén M, Lyngfelt A, Mattisson T, Chen D, Holmen A, Bjørgum E. Novel oxygen-carrier materials for chemical-looping combustion and chemical-looping reforming; LaxSr1−xFeyCo1−yO3−δ perovskites and mixed-metal oxides of NiO, Fe2O3 and Mn3O4. Int J Greenh Gas Control. 2008;2(1):21-36.

101. Johansson M, Mattisson T, Lyngfelt a. Investigation of Mn3O4 With Stabilized ZrO2 for Chemical-Looping Combustion. Chem Eng Res Des. 2006;84(9):807-818.

102. Jerndal E, Mattisson T, Thijs I, Snijkers F, Lyngfelt A. Investigation of NiO/NiAl2O4 oxygen carriers for chemical-looping combustion produced by spray-drying. Int J Greenh Gas Control. 2010;4(1):23-35.

103. Jackson PRS, Young DJ, Trimm DL. Coke deposition on and removal from metals and heat-resistant alloys under steam-cracking conditions. J Mater Sci. 1986;21:4376-4384.

104. Skibbe O, Vogel D, Binder M, et al. Ethene stabilization on Cu(111) by surface roughness. J Chem Phys. 2009;131(2):024701.

105. Choi J-H, Li Z, Cui P, et al. Drastic reduction in the growth temperature of graphene on copper via enhanced London dispersion force. Sci Rep. 2013;3:1925.

106. Li X, Cai W, An J, et al. Large-area synthesis of high-quality and uniform graphene films on copper foils. Science. 2009;324(5932):1312-1314.

107. Chu JH, Kwak J, Kim S-D, et al. Monolithic graphene oxide sheets with controllable composition. Nat Commun. 2014;5:3383.

108. Rabou LPLM, Drift A Van Der. Benzene and ethylene in Bio-SNG production : nuisance , fuel or valuable products? In: *Proceedings of the International Conference on Polygeneration Strategies 11*. Vol ; 2011:157-162.

109. Boerrigter H, Deurwaarder EP, Bergman PCA, van Paasen SVB, van Ree R. Thermal Bio-Refinery; High-Efficient Integrated Production of Renewable Chemicals, (Transportation) Fuels, and Products from Biomass. In: *The 2nd World Conference and Technology Exhibition on Biomass for Energy, Industry and Climate Protection*. Vol ; 2004.

110. Van der Drift B. Chemicals from biomass. In: *IEA/Bioenergy-Task 33 Workshop.* Vol ; 2013.

111. Husmann M, Hochenauer C, Meng X, Jong W De, Kienberger T. Evaluation of sorbents for high temperature in situ desulfurization of biomass-derived syngas. Energy and Fuels. 2014;28:2523-2534.

112. Patrick V, Gavalas GR, Flytzani-Stephanopolous M, Jothimurugesan K. High-temperature sulfidation-regeneration of copper(II) oxide-alumina sorbents. Ind Eng Chem Res. 1989;28:931-940.

113. Hosokai S, Hayashi J-I, Shimada T, et al. Spontaneous Generation of Tar Decomposition Promoter in a Biomass Steam Reformer. Chem Eng Res Des. 2005;83(9):1093-1102.

114. Rabou LPLM, Zwart RWR, Vreugdenhil BJ, Bos L. Tar in biomass producer gas, the Energy research Centre of The Netherlands (ECN) experience: An enduring challenge. Energy and Fuels. 2009;23(12):6189-6198.

115. Yokohawa H. Phase Diagrams and Thermodynamic Properties of Zirconia Based Ceramics. Key Eng Mater. 1998;153-154:37-74.

116. Juutilainen S, Simell P, Krause A. Zirconia: Selective oxidation catalyst for removal of tar and ammonia from biomass gasification gas. Appl Catal B Environ. 2006;62(1-2):86-92.

117. Arjmand M, Leion H, Mattisson T, Lyngfelt A. Investigation of different manganese ores as oxygen carriers in chemical-looping combustion (CLC) for solid fuels. Appl Energy. 2014;113:1883-1894.

118. Gu H, Shen L, Xiao J, Zhang S, Song T, Chen D. Iron ore as oxygen carrier improved with potassium for chemical looping combustion of anthracite coal. Combust Flame. 2012;159(7):2480-2490.

119. Bao J, Li Z, Sun H, Cai N. Continuous Test of Ilmenite-Based Oxygen Carriers for Chemical Looping Combustion in a Dual Fluidized Bed Reactor System. Ind Eng Chem Res. 2013;52(42):14817-14827.

120. Liu L, Zachariah MR. Enhanced Performance of Alkali Metal Doped Fe2O3 and Fe2O3/Al2O3 Composites As Oxygen Carrier Material in Chemical Looping Combustion. Energy and Fuels. 2013;27:4977-4983.

121. Yu Z, Li C, Jing X, et al. Catalytic chemical looping combustion of carbon with an iron-based oxygen carrier modified by K2CO3: Catalytic mechanism and multicycle tests. Fuel Process Technol. 2015;135:119-124.

122. Ge H, Shen L, Gu H, Jiang S. Effect of co-precipitation and impregnation on K-decorated Fe2O3/Al2O3 oxygen carrier in Chemical Looping Combustion of bituminous coal. Chem Eng J. 2015;262:1065-1076.

123. Gu H, Shen L, Zhong Z, et al. Potassium-Modified Iron Ore as Oxygen Carrier for Coal Chemical Looping Combustion : Continuous Test in 1 kW Reactor. Ind Eng Chem Res. 2014;53:13006-13015.

124. Bao J, Li Z, Cai N. Promoting the reduction reactivity of ilmenite by introducing foreign ions in chemical looping combustion. Ind Eng Chem Res. 2013. http://pubs.acs.org/doi/abs/10.1021/ie400237p. Accessed May 1, 2013.

125. Mattisson T, Lyngfelt A, Leion H. Chemical-looping with oxygen uncoupling for combustion of solid fuels. Int J Greenh Gas Control. 2009;3(1):11-19.

126. Lyngfelt A, Leckner B. A 1000MWth boiler for chemical-looping combustion of solid fuels – Discussion of design and costs. Appl Energy. 2015.

127. Linderholm C, Knutsson P, Schmitz M, Markström P, Lyngfelt A. Material balances of carbon, sulfur, nitrogen and ilmenite in a 100kW CLC reactor system. Int J Greenh Gas Control. 2014;27:188-202.

128. Ledin S. Willow wood properties, production and economy. Biomass and Bioenergy. 1996;11(2-3):75-83.

129. Sadeghbeigi R. Fluid Catalytic Cracking Handbook. Vol Third Edit. Butterworth-Heinemann; 2012.

130. Skogsstyrelsen. Wood chips prices in Sweden. 2013. http://www.skogsstyrelsen.se/en/AUTHORITY/Statistics/Subject-Areas/Prices/Tables-and-figures/.

131. Linderholm C, Mattisson T, Lyngfelt A. Long-term integrity testing of spray-dried particles in a 10-kW chemical-looping combustor using natural gas as fuel. Fuel. 2009;88(11):2083-2096.

Appendix: Cost considerations for CLC/DFB/CLR bed materials

When bed materials are used in fluidized bed processes such as the CLC, DFB or CLR processes, not only have materials to be manufactured to comprise the inventory of the reactor, but likely also to provide a continuous make-up stream of bed material to the process during operation. The necessity to provide such a make-up stream to keep the bed inventory constant could derive from

1) the physical loss of bed material due to attrition,
2) the need to maintain bed material reactivity by replacing deactivated bed material with fresh material or
3) mixing of the bed material with ash, and subsequent involuntary removal of the bed material with the ash stream.

When using active metal oxide bed materials in the primary loop (i.e. the DFB gasifier or the CLC unit, see chapter 2), the bed materials are in direct contact with ash and ash-forming minerals introduced to the system via the solid fuel feeding stream. The amount of ash and ash-forming minerals depends of course on the type of solid fuel used, with smaller quantities expected for biomass and large quantities expected for lignite fuels. In any case, as a consequence, intense interaction between the ash and the bed material can be expected. This could potentially lead to deactivation of the bed material and admixing of the bed material and the ash. Therefore, the need for a rather large make-up stream of active bed material can be anticipated. Lyngfelt et al. estimated costs and particle lifetime for a 1000 MW_{th} CLC unit with solid fuel[126]. While attrition data suggested an estimated particle lifetime of 700 h for ilmenite[127], they suggested an expected lifetime of 200 h, or about 8 days, instead due to interaction with ash. Such a short lifetime would put stringent limits on the acceptable costs of the bed material, making the use of cheap ores and natural materials as bed materials attractive (as illustrated in Paper III), while rendering the use of more expensive synthetic materials economically unattractive.

When using active metal oxide bed materials in a secondary loop downstream of the gasifier (i.e. in gas conditioning of raw syngas in a CLR unit, see chapter 3), ash-bed material interaction can be expected to occur in a much lower extent, since a large proportion of ash is commonly separated from the gasification gas by cyclones. The gas introduced to the hot gas conditioning likely still contains significant quantities of dust/ash that could potentially have a deteriorating influence on the bed material performance and lifetime. Nevertheless, the reduced presence of ash and thus the expected reduced deteriorative ash-bed material interaction could potentially increase the lifetime of the bed materials. This increased expected lifetime might generate some economic leeway for the use of more expensive, synthetic bed materials.

The cost of the bed material make-up stream can be illustrated as a function of the average lifetime of the bed material. To determine such cost, the bed inventory needs to be approximated. Herein, an attempt is made to approximate the bed inventory of a CLR process downstream of a DFB gasifier with a 100 MW_{th} biomass input, under the following assumptions:

- DFB process with 100 MW_{th} dry wood chips input with heating value of 19 MJ/kg[128]
- Steam-to-Fuel ratio of 0.8 kg/kg in the gasifier
- A fuel conversion in the gasifier of 85 wt-%, the remainder being burned in combustor
- Molar mass of gasification gas M=20.6 g/mol, corresponding to Chalmers gasifier gas composition (see Table 2)
- Resulting gas flow rate from gasifier V_N=10 m^3_N/s
- Target GHSV= 2500 h^{-1}. At this GHSV, a high degree of benzene conversion of 90% should be attainable with Fe,Sr doped $La_2Zr_2O_7$ supported on ZNANO at T=850°C (see Figure 20)
- Bulk density of the bed material 0.93 g/ml, corresponding to Fe,Sr doped $La_2Zr_2O_7$ supported on ZNANO
- Bed volume of the regenerator negligible in comparison to the reformer

With these assumptions a required bed inventory of approximately 13 tons for the CLR downstream of a 100 MW_{th} DFB plant can be calculated. Further assuming a plant availability of 100 %, the yearly cost for the makeup stream of bed material can be calculated as a function of the particle lifetime and the specific cost of the bed material. Such a cost prediction is shown in Figure 24.
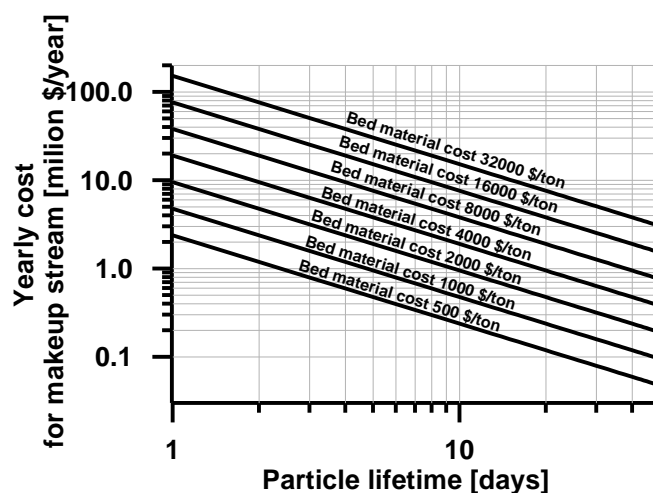
Figure 24. Predicted yearly cost for bed material makeup stream for 100 MW_{th} fuel input plant as function of particle lifetime and with specific bed material cost as parameter.

As a point of reference, one can consider the FCC process as a process that the CLR process shares many common characteristics with. In the FCC process the cost of the zeolite catalytic bed material is usually in the range of about 4000 $/ton[129], and the daily makeup rate is typically between 1-2 % of the inventory, leading to a particle lifetime of 50-100 days[129]. For a conservative estimate of 50 days of particle lifetime, this would result in a yearly cost for the makeup stream of the 100 MW$_{th}$ plant of about 380,000 $.

To provide a reference scale for these costs, the cost for the makeup stream can also be expressed as a fraction of the fuel cost of the plant. Assuming the fuel to be Swedish wood chips at a cost of 200 SEK/MWh or 24 $/MWh[130], the yearly fuel cost of a 100 MW$_{th}$ plant would amount to about 21 million $. For the FCC bed material, under the assumptions stated above, the makeup stream of bed material would thus amount to about 1.8 % of the fuel costs.

For the bed materials investigated in this work, such as the Fe,Sr-doped $La_2Zr_2O_7$ supported on ZrO_2, a higher specific cost needs to be expected due to the comparatively high cost of ZrO_2 as support material and the presumably higher production costs due to a smaller scale production. As of yet, it is unclear what particle lifetimes are to be expected for CLR units. Lifetime predictions for CLC units operated with rather clean natural gas as a fuel indicated that, for spray-dried $NiO/NiAl_2O_4$ particles, lifetimes of up to 33,000 h (1375 days) might be achievable if only the physical loss of bed material due to particle disintegration is considered[131]. However, it is doubtful whether such long particle lifetimes can be achieved when a raw, dusty, contaminant-laden gasification gas is to be reformed. Under such conditions, attrition might not be the lifetime-limiting factor any longer. Nonetheless, given that a reasonably long particle lifetime can be achieved, it appears feasible to utilize even rather expensive synthetic bed materials in a CLR unit.